PLOS GENETICS

RESEARCH ARTICLE

A forward genetic screen identifies Dolk as a regulator of startle magnitude through the potassium channel subunit Kv1.1

Joy H. Meserve[1], Jessica C. Nelson[1], Kurt C. Marsden[1¤a], Jerry Hsu[1], Fabio A. Echeverry[2], Roshan A. Jain[1¤b], Marc A. Wolman[1], Alberto E. Pereda[2], Michael Granato[1]*

1 Department of Cell and Developmental Biology, Perelman School of Medicine, University of Pennsylvania, Philadelphia, Pennsylvania, United States of America, **2** Dominick P. Purpura Department of Neuroscience, Albert Einstein College of Medicine, Bronx, New York, United States of America

¤a Current address: Department of Biological Sciences, North Carolina State University, Raleigh, North Carolina, United States of America
¤b Current address: Department of Biology, Haverford College, Haverford, Pennsylvania, United States of America
* granatom@pennmedicine.upenn.edu

Citation: Meserve JH, Nelson JC, Marsden KC, Hsu J, Echeverry FA, Jain RA, et al. (2021) A forward genetic screen identifies Dolk as a regulator of startle magnitude through the potassium channel subunit Kv1.1. PLoS Genet 17(6): e1008943. https://doi.org/10.1371/journal.pgen.1008943

Editor: Cecilia Moens, Fred Hutchinson Cancer Research Center, UNITED STATES

Received: June 15, 2020

Accepted: May 4, 2021

Published: June 1, 2021

Data Availability Statement: All relevant data are within the manuscript and its Supporting Information files.

Funding: This work was supported by NIH (R01MH109498 and R01NS118921 to MG, F32MH115434 to JHM, and R01DC011099 to AEP). The funders had no role in study design, data collection and analysis, decision to publish, or preparation of the manuscript.

Competing interests: The authors have declared that no competing interests exist.

Abstract

The acoustic startle response is an evolutionarily conserved avoidance behavior. Disruptions in startle behavior, particularly startle magnitude, are a hallmark of several human neurological disorders. While the neural circuitry underlying startle behavior has been studied extensively, the repertoire of genes and genetic pathways that regulate this locomotor behavior has not been explored using an unbiased genetic approach. To identify such genes, we took advantage of the stereotypic startle behavior in zebrafish larvae and performed a forward genetic screen coupled with whole genome analysis. We uncovered mutations in eight genes critical for startle behavior, including two genes encoding proteins associated with human neurological disorders, Dolichol kinase (Dolk), a broadly expressed regulator of the glycoprotein biosynthesis pathway, and the potassium Shaker-like channel subunit Kv1.1. We demonstrate that Kv1.1 and Dolk play critical roles in the spinal cord to regulate movement magnitude during the startle response and spontaneous swim movements. Moreover, we show that Kv1.1 protein is mislocalized in *dolk* mutants, suggesting they act in a common genetic pathway. Combined, our results identify a diverse set of eight genes, all associated with human disorders, that regulate zebrafish startle behavior and reveal a previously unappreciated role for Dolk and Kv1.1 in regulating movement magnitude via a common genetic pathway.

Author summary

Underlying all animal behaviors are neural circuits, which are controlled by numerous molecular pathways that direct neuron development and activity. To identify and study the molecular pathways that control behavior, we use a simple vertebrate behavior, the

acoustic startle response, in the larval zebrafish. In response to an intense noise, larval zebrafish will quickly turn and swim away to escape. From a genetic screen, we have identified a number of mutants that behave in abnormal ways in response to an acoustic stimulus. We cloned these mutants and identified eight genes that regulate startle behavior. All eight genes are associated with human disorders, and here we focus on two genes, *dolk* and *kcna1a*, encoding Dolk, a key regulator of protein glycosylation, and the potassium channel subunit Kv1.1, respectively. We demonstrate that loss of *dolk* or *kcna1a* causes larval zebrafish to perform exaggerated swim movements, and Dolk is required for Kv1.1 protein localization to axons of neurons throughout the nervous system, providing strong evidence that *dolk* and *kcna1a* act in a common molecular pathway. Combined, our studies provide new insights into the genetic regulation of startle behavior.

Introduction

Defects in initiating or executing movements are associated with a range of disorders. While some neurological disorders are primarily defined by motor impairments, several disorders defined primarily by cognitive deficits include motor features. For example, the eyeblink response, in which a patient reacts to a startling stimulus, is disrupted in a variety of neurodevelopmental and psychiatric disorders, including obsessive compulsive disorder, schizophrenia, posttraumatic stress disorder, and autism spectrum disorder [1–4]. The eyeblink response is one component of the startle response, which in humans is a whole-body defensive maneuver to shield the upper body from impact and in aquatic vertebrates, including zebrafish, is critical to evade avoid predators [5,6]. A combination of electrophysiological, lesion, and imaging studies have uncovered the core neural circuity underlying startle behavior in human and various vertebrate animal models [7–10]. Yet despite its critical role in animal survival and its link to several neurological disorders, the repertoire of genes and genetic pathways that regulate startle behavior has not been explored using an unbiased genetic approach.

Over the past several decades, the larval zebrafish has emerged as a powerful vertebrate model organism for unbiased genetic screens to identify genes critical for basic locomotion [11–13] and more recently for more complex behaviors, including visual behaviors and sleep [14,15]. However, an unbiased genetic screen to identify the genes critical for the execution of the startle response has been absent. By five days post fertilization (dpf), in response to an acoustic stimulus, zebrafish larvae undergo a characteristic short latency C-start (SLC), consisting of a sharp C-shaped turn and swimming away from the stimulus [16] (Fig 1B–1F and S1 Video). The behavioral circuit for the acoustic startle response is well characterized (reviewed in [9,17], Fig 1A) and is functionally similar to the human startle circuit [5]. Central to the zebrafish acoustic startle circuit are the Mauthner cells, a bilateral pair of reticulospinal neurons in the hindbrain. The Mauthner cells are necessary and sufficient for this short latency escape behavior [16,18,19]. Hair cell activation following an acoustic stimulus leads to activation of the eighth cranial nerve, which, along with the spiral fiber neurons, provides excitatory input to the Mauthner cell. The Mauthner cell directly activates contralateral primary motor neurons and excitatory interneurons to drive unilateral body contraction and turning away from the acoustic stimulus [20,21]. Inhibitory input prevents Mauthner cell firing at subthreshold stimuli or when the other Mauthner cell has already fired [22]. Because the circuit is well defined and the behavior is robust, this system is ideal for investigating how genes regulate behavior.

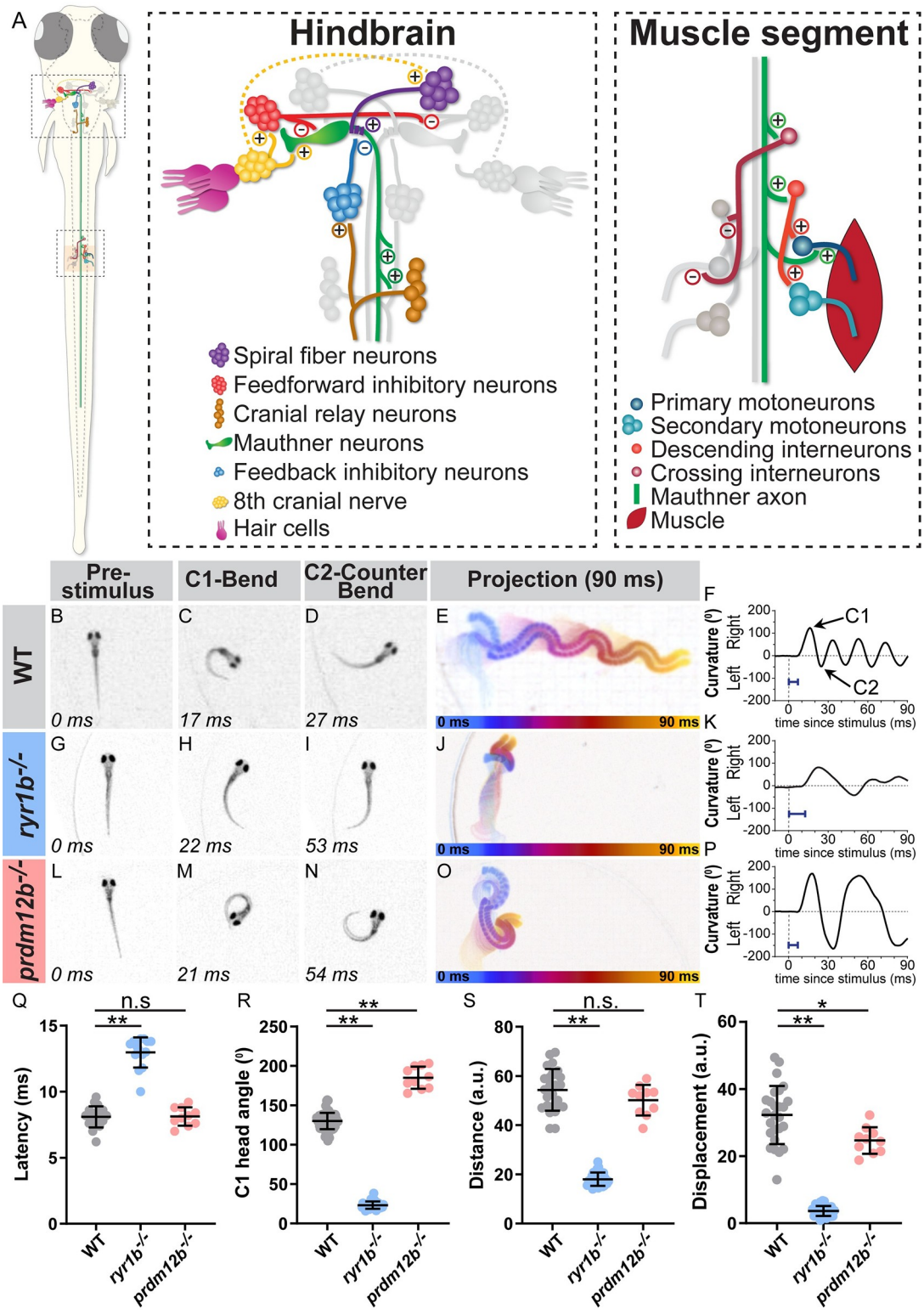

Fig 1. The zebrafish larval startle response is amenable to circuit and genetic analysis. (A) The acoustic startle response is driven by an action potential from the Mauthner neuron (green), which activates motor neurons in the spinal cord to drive a contralateral body bend. Excitatory and inhibitory neurons in the hindbrain and in the spinal cord impinge upon the Mauthner cells to ensure motor neurons fire on only one side. (B-F) A representative acoustic startle response in a 5 dpf (days post fertilization) wild type larva. An acoustic stimulus is delivered at 0 ms (B), which elicits a rapid turn (C) followed by a counter

bend (D) and swimming away (projection of 90 ms response in E, color coded by time). Automated tracking of the curvature of the larva throughout the behavior (F) reveals the response latency (blue bar = latency in F,K,P). (G-K) *ryr1b* mutants display a weak startle response with reduced bend and counter bend angles (H,I) and reduced displacement (J), largely due to minimal swimming after the counter bend (K). (L-P) *prdm12b* mutants display an exaggerated startle response with increased bend and counter bend angles (M,N). The duration of each bend is longer than in wild type as well (P). (Q-T) Quantification of response latency (Q; manual measurement); max C1 head angle (R; automated measurement); distance traveled along escape trajectory (S; automated measurement); and displacement from initial head position to final head position (T; automated measurement). Each point is the average response over ten trials for an individual larva. $n \geq 10$ larvae, $^{*}p = 0.002$, $^{**}p < 0.0001$ (one-way ANOVA with Tukey correction for multiple comparisons).

https://doi.org/10.1371/journal.pgen.1008943.g001

We previously performed a forward genetic screen to identify functional regulators of the acoustic startle response. This approach identified a distinct set of genes with previously unrecognized roles critical for startle habituation [23,24], startle sensitivity [25], and sensorimotor decision making [26]. Here, we describe kinematic mutants identified from this screen that display defects in executing swim movements of the startle response. These mutants fall into two general categories. One group of mutants display a "weak" acoustic startle response characterized by shallow bends and minimal displacement. Using high-throughput sequencing, we have identified causative mutations in five weak startle mutants. In all five lines, the affected genes control muscle or neuromuscular junction (NMJ) function and are associated with locomotor disorders in humans.

The second group of mutants perform high amplitude bends, resulting in an "exaggerated" response. For one of the exaggerated startle mutant lines, we identified a causative mutation in *PR domain containing 12b* (*prdm12b*), a transcription factor that controls development of inhibitory neurons in the spinal cord and has previously been shown to be important for regulation of movement in fish [27]. The remaining two exaggerated mutant lines harbor mutations in *dolichol kinase* (*dolk*), which encodes a glycosylation pathway enzyme, and in *potassium voltage-gated channel*, *shaker-related subfamily*, *member 1a* (*kcna1a*), which encodes the potassium channel subunit Kv1.1. We demonstrate that *dolk* and *kcna1a* likely act in a common pathway to control startle movement magnitude as Dolk is required for Kv1.1 protein localization. Additionally, we demonstrate that Kv1.1 and Dolk act in the spinal cord to control the magnitude of body bends. Thus, through our forward genetic screen we identified a number of genes that are essential to regulate body movement. Furthermore, we demonstrate how a broadly expressed protein, Dolk, selectively regulates behavior through the Kv1.1 protein.

Results

A forward genetic screen for regulators of the larval startle response

We previously performed a forward genetic screen for regulators of the acoustic startle response [23–26]. In brief, using a high-speed camera and automatic tracking, individual F3 larvae were exposed to a series of startling stimuli (for details on mutagenesis and the breeding scheme to obtain F3 larvae see [23]). This portion of the screen focused on kinematic mutants, characterized by significant changes in any of the stereotypic parameters characteristic of the startle response (Table 1). Putative mutant lines were retested in the subsequent generation to confirm genetic inheritance. This screen identified a group of eight mutants defective in kinematic parameters (including response latency, turn angle, distance, and displacement). These mutants fall into two categories: five mutant lines display shallow bends of decreased turning angle compared to their siblings (one representative mutant line shown in in Fig 1G–1K and 1Q–1T, S2 Video); we refer to these as "weak" startle mutants. Three mutant lines perform numerous high amplitude bends in response to an acoustic stimulus. These turns often result

Table 1. Genes identified from a forward genetic screen that regulate locomotor behaviors in larval zebrafish.

Gene[allele]	Mutation	Assoc. Disorder [OMIM Gene Entry]	Latency (ms)	C1 Angle (^{0})	Distance (a.u.)	Displace- ment (a.u.)	Spont. Mov. Distance (a.u.)
neb^{p413}	Y4366*	nemaline myopathy [161650]	10.8 ± 0.8,* 134% of sibs	22.1 ± 6.0,* 18% of sibs	18.1 ± 4.7,* 30% of sibs	5.1 ± 2.4,* 13% of sibs	209.0 ± 78.2,* 18% of sibs
ryr1b^{p414}	SPLICE SITE†	multi-minicore disease [180901]	13.0 ± 1.1,* 141% of sibs	23.2 ± 4.7,* 22% of sibs	18.0 ± 2.7,* 29% of sibs	3.7 ± 1.5,* 8% of sibs	894.0 ± 612.6,$^{n.s.}$ 94% of sibs
cacna1ab^{p415}	Y517*	episodic ataxia, type 2 [601011]	24.1 ± 3.3,* 278% of sibs	39.9 ± 8.4,* 32% of sibs	28.7 ± 3.5,* 46% of sibs	12.0 ± 4.0,* 29% of sibs	506.0 ± 346.0,* 33% of sibs
rapsn^{p416}	K60*	myasthenic syndrome [601592]	9.1 ± 1.0,$^{n.s.}$ 106% of sibs	91.1 ± 13.2,* 78% of sibs	37.3 ± 3.1,* 62% of sibs	16.4 ± 3.6,* 40% of sibs	198.9 ± 132.8,*13% of sibs
slc5a7a^{p417}	W202*	distal hereditary motor neuropathy [608761]	12.0 ± 1.2,* 142% of sibs	67.1 ± 38.6,* 52% of sibs	27.6 ± 7.2,* 43% of sibs	7.1 ± 5.0,* 16% of sibs	76.7 ± 74.4,* 4%, of sibs
prdm12b^{p419}	L197P	hereditary sensory and autonomic neuropathy VIII [616458]	8.1 ± 0.7,$^{n.s.}$ 96% of sibs	185 ± 14.0,* 165% of sibs	50.2 ± 6.2,$^{n.s.}$ 92% of sibs	24.66 ± 3.9,* 76% of sibs	1188.3 ± 989.7,$^{n.s.}$ 96% of sibs
dolk^{p420}	W25*	congenital disorder of glycosylation [610746]	15.5 ± 1.5,* 155% of sibs	160.5 ± 14.7,* 153% of sibs	62.2 ± 6.0,* 110% of sibs	15.8 ± 2.0,* 44% of sibs	681.7 ± 438.1,* 48% of sibs
kcna1a^{p181}	N250K	episodic ataxia/myokymia syndrome [176260]	11.0 ± 1.7,* 116% of sibs	159.3 ± 12.9,* 128% of sibs	69.4 ± 5.6,* 121% of sibs	18.8 ± 4.5,* 51% of sibs	499.8 ± 463.6,* 31% of sibs

Behavioral characteristics of kinematic mutant larvae. Mutations causing "weak" startle responses are shaded in blue. Mutations causing "exaggerated" startle responses are shaded in red. Averages (±SD) are presented from at least ten sibling larvae and ten mutant larvae per genotype over ten acoustic stimulus trials or over one minute of spontaneous movement.

*$p<0.01$ (Mann-Whitney tests).

†Splice donor after exon 4 mutated so intron retained; premature stop five codons into intron.

https://doi.org/10.1371/journal.pgen.1008943.t001

in larvae swimming in a figure eight pattern (one representative mutant line shown in Fig 1L–1T and S3 Video); we refer to these as "exaggerated" startle mutants. Combined, these eight mutant lines offer an opportunity to reveal genetic regulators of movement kinematics.

To identify the molecular mechanisms underlying these behavioral phenotypes, we first set out to identify the causative mutations. In all kinematic mutant lines, approximately 25% of progeny from carrier incrosses display the mutant behavioral phenotype, consistent with the causative mutations being recessive, monoallelic, and causing highly penetrant phenotypes. In addition, when behaviorally mutant larvae were raised for each of seven lines, no animals survived past two weeks, indicating these lines harbor homozygous lethal mutations. For the eighth line (*kcna1a*^{p181}), we found rare escapers (~5%) that lived >two months, but these fish did not grow past a juvenile stage (<1 cm in length). This lethality can likely be attributed to defects with swimming and hence deficits in prey capture and feeding. For each mutant line, after behavioral testing, pools of behaviorally mutant larvae and behaviorally wild type siblings were collected for high-throughput DNA sequencing. We performed whole genome sequencing (WGS) and homozygosity analysis on mutant and sibling pools for four of the lines, as described in more detail in [23]. Using known single nucleotide polymorphisms (SNPs) present in our wild type background, we identified regions of homozygosity in the mutant pools that were heterozygous in the sibling pool. Within these regions of homozygosity, potentially detrimental exonic SNPs not observed in wild type fish were identified. Nonsense mutations, particularly in genes known to function in neurons or muscle, were prioritized. Individual larvae displaying mutant or wild type behavior were then sequenced for potentially causative SNPs. If a potential SNP was observed as homozygous in 100% of mutant larvae (>20 individuals) and heterozygous or homozygous wild type in all siblings (>20 individuals), we considered the SNP to likely be causative. For the remaining four mutant lines, we performed whole

exome sequencing (WES) [28]. To identify linkage (SNPs with allelic frequencies ~100% in mutants and ~33% in siblings, based on ratio of heterozygous to homozygous wild type larvae) and potentially causative mutations, we used the online tool SNPTrack [29]. Confirmation of potentially causative mutations was performed as described above for candidates from WGS. Five lines (*neb*, *cacna1ab*, *ryr1b*, *rapsn*, and *slc5a7a*) contain nonsense mutations (or a splice mutation resulting in nonsense mutation) in genes known to regulate neuron or muscle function (see Table 1), strongly indicating we have identified the correct mutation (see also discussion of identified genes below). Two of the mutant lines (*prdm12b* and *kcna1a*) have missense mutations, and we or others have generated nonsense alleles that display the same phenotype. For the remaining mutant line (*dolk*) containing a nonsense mutation, we generated an independent second mutant allele to confirm that mutations in *dolk* are causative for the exaggerated locomotor phenotype (see below). Based on these data, we are confident we have identified mutant alleles of eight genes critical for regulating proper kinematic behavior during the acoustic startle response. We note that all genes have a human disease associated counterpart and that six of the eight genes are associated with human movement disorders, further underscoring conservation of disease associated genes in zebrafish [30] (Table 1). Based on their molecular identities, the affected genes can be subdivided by their likely site of action. Below, we report on several genes that act in skeletal muscle, at the neuromuscular junction, or in inhibitory spinal neurons, and we then focus on two genes likely to act in the same pathway to regulate movement magnitude.

Genes controlling muscle function modulate acoustic startle kinematics

Of the five weak startle mutant lines, two have mutations in genes that are required for muscle function. *p413* mutants contain a nonsense mutation in the *nebulin* (*neb*) gene (Table 1), which encodes a protein necessary for sarcomere assembly and subsequent function [31]. Previous work in zebrafish demonstrated that a loss-of-function *neb* allele displays defects in sarcomere assembly, leading to reduced swim movement [32]. The second mutant line we identified, *p414*, contains a splice mutation in the *ryanodine receptor 1b* (*ryr1b*) gene (Table 1 and Fig 1G–1K and 1Q–1T). RyR1 is required for calcium release at the sarcoplasmic reticulum, which drives muscle contraction. A previously characterized zebrafish allele of *ryr1b*, called *relatively relaxed*, displays a decreased touch response and reduced Ca^{2+} transients in fast muscle [33]. Interestingly, RyR1b is expressed primarily in fast muscle while RyR1a is expressed primarily in slow muscle [33]. Consistent with this finding, $ryr1b^{p414}$ mutants display a drastic startle response defect, which is dependent on fast muscle. However, spontaneous movement, which is dependent on slow muscle, is not significantly different from siblings (Table 1). This result emphasizes the importance of examining different behaviors, especially ones that utilize different circuitry and muscle groups [20,34,35], when characterizing locomotion in mutant animals.

Genes acting at the neuromuscular junction regulate acoustic startle kinematics

Three genes identified in our screen are required at the neuromuscular junction (NMJ). This includes a new mutant allele, *p416*, of the gene *receptor-associated protein of the synapse* (*rapsn*), originally identified as *twitch once* mutants [11], and subsequently shown to be caused by mutation in the *rapsn* locus [36]. *rapsn* mutants display reduced spontaneous swimming and touch responses [11] caused by decreased acetylcholine receptor clustering at NMJs [36]. In addition, we identified a nonsense mutation (*p415*) in the *calcium channel*, *voltage-dependent*, *P/Q type*, *alpha 1A subunit*, *b* (*cacna1ab*) gene, which encodes $Ca_v2.1$. A previously

identified mutant allele of *cacna1ab*, *fakir*, displays a weak touch response [11,37]. This weak touch response in *fakir* larvae can be attributed to defects in transmission at the NMJ [38]. This likely accounts for the reduction in startle response and spontaneous movement we observe in *p415* (Table 1). Since *rapsn* and *cacna1ab* were both previously identified in a screen for escape response following a tail touch [11], which is driven by the Mauthner cells [39], we predicted they could be identified in the Mauthner-dependent acoustic startle screen described here.

The fifth weak startle mutant, *p417*, demonstrates a unique behavior (S1 Fig). Unlike sibling larvae that initiate the startle response at the head (S1C–S1G Fig), in *p417* mutants, the startle response often initiates with a turn in the tail instead (S1H–S1L Fig and S4 Video). Subsequent body bends are uncoordinated, rather than a smooth progression from head to tail. The C1 angle, distance, and displacement are also drastically reduced in these mutants, and mutants undergo very little spontaneous movement (Table 1). We identified the causative *p417* mutation as a nonsense mutation in *slc5a7a*, which encodes the high-affinity choline transporter (CHT) (S1A and S1B Fig). Uptake of choline by the high-affinity choline transporter is the rate limiting step for acetylcholine synthesis [40], so Slc5a7 is essential for cholinergic transmission.

There are a number of cholinergic neuronal populations in the acoustic startle circuit. Most notably, spinal motor neurons release acetylcholine at the NMJ to activate skeletal muscle in the trunk and tail [41]. We hypothesized the *slc5a7a* mutant phenotype of reduced turn angle and minimal displacement is caused by reduced muscle contractions due to reduced acetylcholine release at the NMJ. To test this, we generated a transgenic line in which *slc5a7a* is expressed under the control of a motor neuron specific promoter, *mnx1/hb9* [42] (S1M Fig). Compared to *slc5a7a* mutants lacking the transgene (S1N–S1P Fig), mutant larvae expressing the transgene (*slc5a7a*$^{-/-}$*; Tg(hb9:slc5a7a)*, display a significantly increased turn angle and distance traveled following an acoustic stimulus. Thus, motor neuron specific expression of *slc5a7a* partially rescues the mutant phenotype, providing strong evidence that Slc5a7a plays a critical role in regulating coordinated swim movements, presumably by increasing acetylcholine level release at NMJs.

prdm12b regulates development of V1 interneurons and modulates acoustic startle kinematics

In addition to the five weak startle mutants described above, we identified three exaggerated startle mutants. In the *p419* mutant line in which the C1 turning angle of the startle response is dramatically increased (165% of wild type siblings; Table 1 and Fig 1L–1P and S3 Video), we identified a missense mutation in the coding sequence of *PR domain containing 12b* (*prdm12b*). Prdm proteins are transcription factors, and several family members have been shown to play roles in nervous system development [43]. Zebrafish *prdm12b* was previously identified in a screen for genes that express in the nervous system [44]. Morpholinos targeting *prdm12b* [27] and a *prdm12b* CRISPR mutation [45] result in larvae with aberrant, exaggerated touch behaviors, similar to the exaggerated acoustic startle response we observe in the *p419* mutants. *prdm12b* is required for development of *engrailed 1b* positive, V1 interneurons in the spinal cord [27]. V1 interneurons are glycinergic and have been shown to regulate the speed of locomotor movements in mammals [46]. In zebrafish larvae, ablation of V1 interneurons results in an exaggerated touch response [47], reminiscent of the exaggerated startle response we observe in *prdm12b* mutants. Thus, Prdm12b is required during development for the specification of inhibitory spinal neurons utilized for the acoustic startle response to achieve coordinated and controlled movement.

The glycosylation pathway protein Dolk regulates acoustic startle magnitude

In a second exaggerated movement mutant, *p420*, we identified a nonsense mutation in the *dolichol kinase* (*dolk*) gene (Fig 2A and 2B). Similar to *prdm12b* mutants, the *dolk* mutant C1 turn angle is dramatically increased (153% of wild type siblings; Table 1 and Fig 2C–2M). In addition to exaggerated C1 turn angles in response to an acoustic stimuli, *dolk* mutants swim in "figure eights," resulting in reduced displacement (Fig 2K and 2O). Dolk catalyzes the CTP-dependent phosphorylation of dolichol to dolichol monophosphate. Dolichol monophosphate

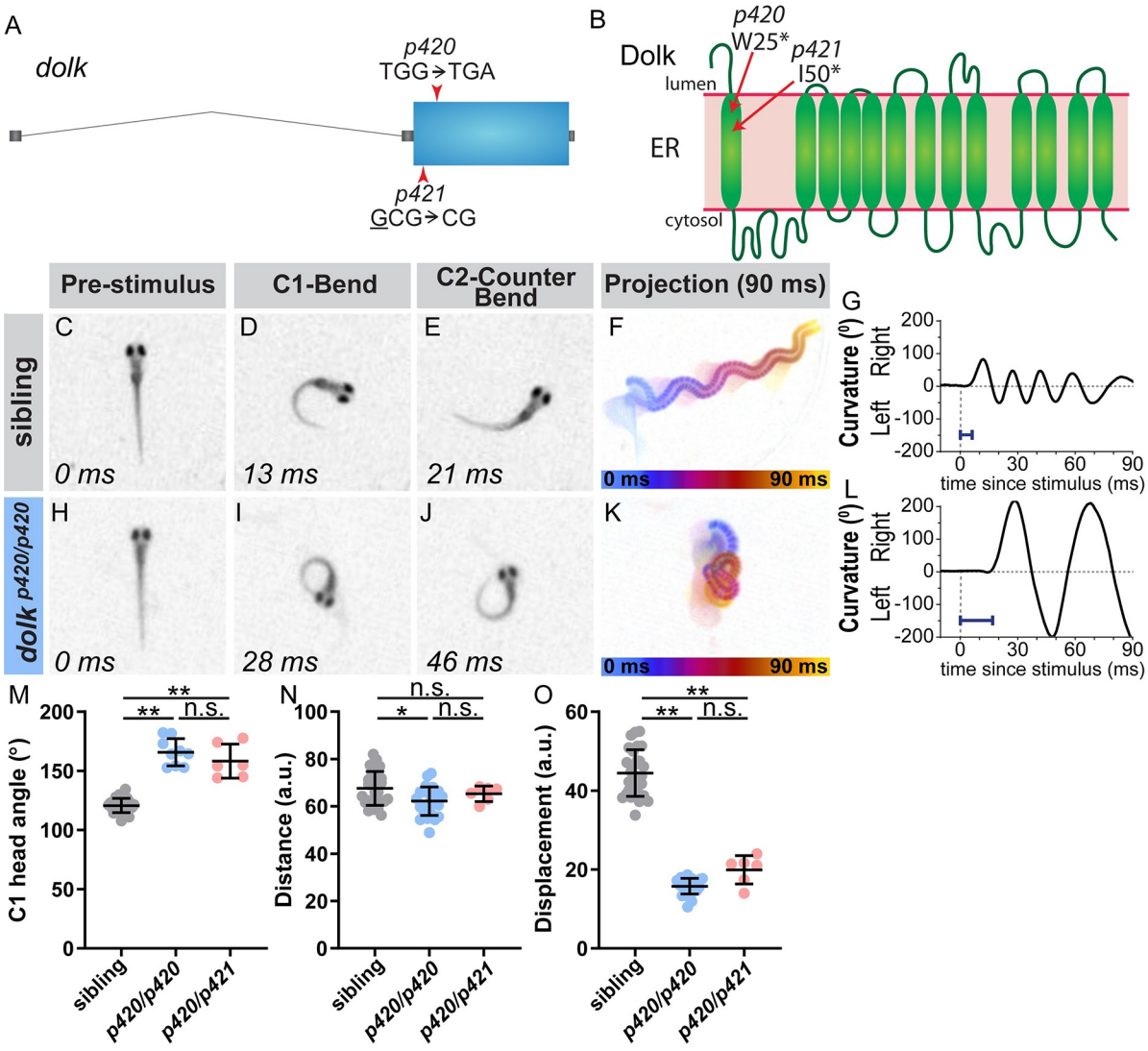

Fig 2. The glycosylation pathway enzyme Dolk regulates the magnitude of the startle response. (A) Gene structure for *dolk* with the nonsense mutation from the screen noted (*p420*). The CRISPR 1 bp deletion allele is also noted (*p421*). (B) Protein structure for Dolk on the endoplasmic reticulum [48], with the predicted amino acid change from the screen mutation indicated. The deletion in the CRISPR allele causes a frame shift in the sequence that results in a premature stop at amino acid 50. In contrast to siblings (C-G), *dolk* mutants (H-L) display an exaggerated startle response, with an increased bend and counter bend angle (I,J), resulting in larvae swimming in a "figure eight" (K). Blue bar = latency in G,L. (M-O) Kinematic parameters of the acoustic startle response in *dolk* siblings and mutants (homozygotes of the screen identified mutation, *p420/p420*, and transheterozygotes from the screen mutation and CRISPR, *p420/p421*). Each point represents average of ten trials for an individual fish. n≥6 larvae, $^{**}p<0.001$, $^{*}p = 0.008$ (one-way ANOVA with Tukey correction for multiple comparisons).

https://doi.org/10.1371/journal.pgen.1008943.g002

is an essential glycosyl carrier for C- and O-mannosylation and N-glycosylation of proteins [48]. To confirm that the *dolk* nonsense mutation identified in our screen (*p420*) is causative, we generated a second mutant *dolk* allele using CRISPR/Cas9. In this *dolk* ^{p421} CRISPR allele, a 1 bp deletion results in a frameshift and premature stop codon at position 50. Both mutations occur early in the protein sequence (Fig 2B), and we predict they likely eliminate all protein function. Transheterozygous (*p420/p421*) *dolk* mutants display the same exaggerated phenotype as *p420* homozygotes (Fig 2M–2O), confirming that mutations in *dolk* cause the behavioral deficits observed in the original *p420* mutants.

The potassium channel subunit Kv1.1 regulates acoustic startle magnitude

Given Dolk's critical role in protein glycosylation, we predict that in *dolk* mutants, many proteins exhibit reduced glycosylation. In 2 dpf zebrafish, over 160 unique glycosylated proteins have previously been cataloged via mass spectrometry [49], so predicting the number and identities of Dolk's behavior-relevant glycosylation targets is challenging. To identify the relevant glycosylated downstream protein(s), we instead turned to our remaining exaggerated mutant line. In this line, we identified a missense mutation in *kcna1a*, which encodes the voltage potassium Shaker-like channel subunit Kv1.1 (Fig 3A and 3B). We have previously characterized this allele for its role in regulating startle habituation [24]. Cell culture studies have shown that Kv1.1 is highly glycosylated, and glycosylation is required for Kv1.1 channel function [50–52]. We confirmed the kinematic defect in the screen *p181* allele (Fig 3C–3O) is due to the missense mutation in *kcna1a* using a previously generated *kcna1a* CRISPR allele (*p410*), which harbors an early stop codon and is a presumed null [24]. *p181/p410* transheterozygotes display the same exaggerated movements as mutants homozygous for *p181* (Fig 3M–3O), and *p181* homozygous larvae are behaviorally not significantly different from *p410* homozygous larvae (Fig 3M–3O). Combined, this strongly suggests that the screen missense *p181* allele also represents a null allele for the kinematic behavior. Thus, *kcna1a* and *dolk* are both required for executing controlled movements, possibly via Dolk-dependent glycosylation of Kv1.1.

Dolk is required for axonal localization of Kv1.1

Glycosylation is well known to regulate protein activity, localization, and/or stability [53]. To address whether *dolk* is critical for Kv1.1 localization or stability, we examined Kv1.1 protein localization in *dolk* mutants using a previously validated antibody [24]. In mammals, Kv1.1 is broadly expressed throughout the brain and primarily localizes to axons and axon terminals [54]. In 5 dpf wild type larvae, we observe Kv1.1 protein localization to axon tracts throughout the brain (Fig 4A and 4B) and the spinal cord (Fig 4C). Kv1.1 strongly accumulates at the Mauthner axon cap (Fig 4B), where spiral fiber and inhibitory neurons synapse onto the Mauthner axon initial segment (AIS). In contrast, in *dolk* mutants, Kv1.1 protein localization is strongly reduced or absent in axon tracts and instead is prominent in somata throughout the brain and spinal cord (Fig 4D–4G). This is particularly apparent in the large Mauthner soma (Fig 4E and 4F). Little or no Kv1.1 is detectable at the axon cap (Fig 4E and 4F) in *dolk* mutants. Since we do still observe Kv1.1 expression in *dolk* mutants, Dolk may be largely dispensable for Kv1.1 protein stability yet indispensable for correct Kv1.1 cell surface localization. This might reflect an indirect role of Dolk on Kv1.1 localization via additional Dolk glycosylation targets. Alternatively, this might reflect a more direct role of Dolk-dependent glycosylation on Kv1.1 localization (see Discussion). As previous studies have shown that Kv1.1 membrane localization is required for its channel function, the most parsimonious explanation for the behavioral phenotype in *dolk* mutants is the lack of proper Kv1.1 localization.

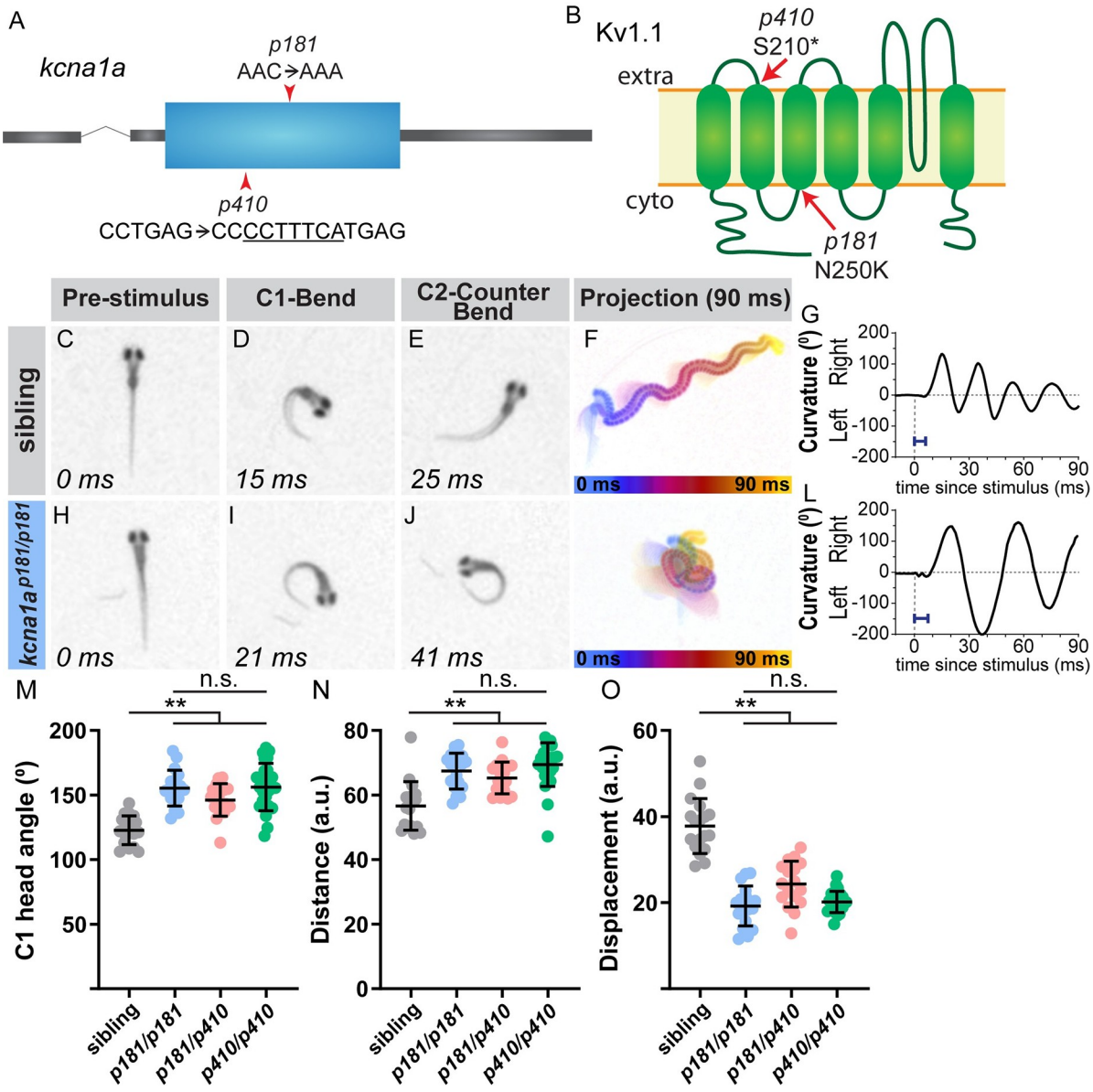

Fig 3. The potassium channel subunit Kv1.1 regulates the magnitude of the startle response. (A) Gene structure for *kcna1a* with the missense mutation from the screen noted (*p181*). The CRISPR 7 bp insertion allele is also noted (*p410*). (B) Protein structure for Kv1.1, which is encoded by *kcna1a*, on the plasma membrane, with the predicted amino acid change from the screen allele (*p181*) indicated. The insertion in the CRISPR allele (*p410*) causes a frame shift in the sequence that results in a premature stop at amino acid 210. In contrast to siblings (C-G), *kcna1a* mutants (H-L) display an exaggerated startle response, with an increased bend and counter bend angle (I,J), resulting in fish swimming in a "figure eight" (K). Blue bar = latency in G,L. (M-O) Kinematic parameters of the acoustic startle response in *kcna1a* sibling and mutants (homozygotes of the screen mutation, *p181/p181*, transheterozygotes of the screen mutation and CRISPR, *p181/p410*, and homozygotes of the CRISPR mutation, *p410/p410*). Each point represents average of ten trials for an individual fish. n≥17 larvae, $^{**}p<0.001$ (one-way ANOVA with Tukey correction for multiple comparisons).

https://doi.org/10.1371/journal.pgen.1008943.g003

Kv1.1 acts in the spinal cord to regulate swim movement magnitude

We next asked where in the startle circuit Kv1.1 acts to regulate the magnitude of the startle response. Expression of Kv1.1 throughout the hindbrain and spinal cord is consistent with the idea that Kv1.1 may act at various sites in the startle circuit. *kcna1a* mRNA is observed in Mauthner neurons as early as 2 dpf, and developmental expression of Kv1.1 correlates with the

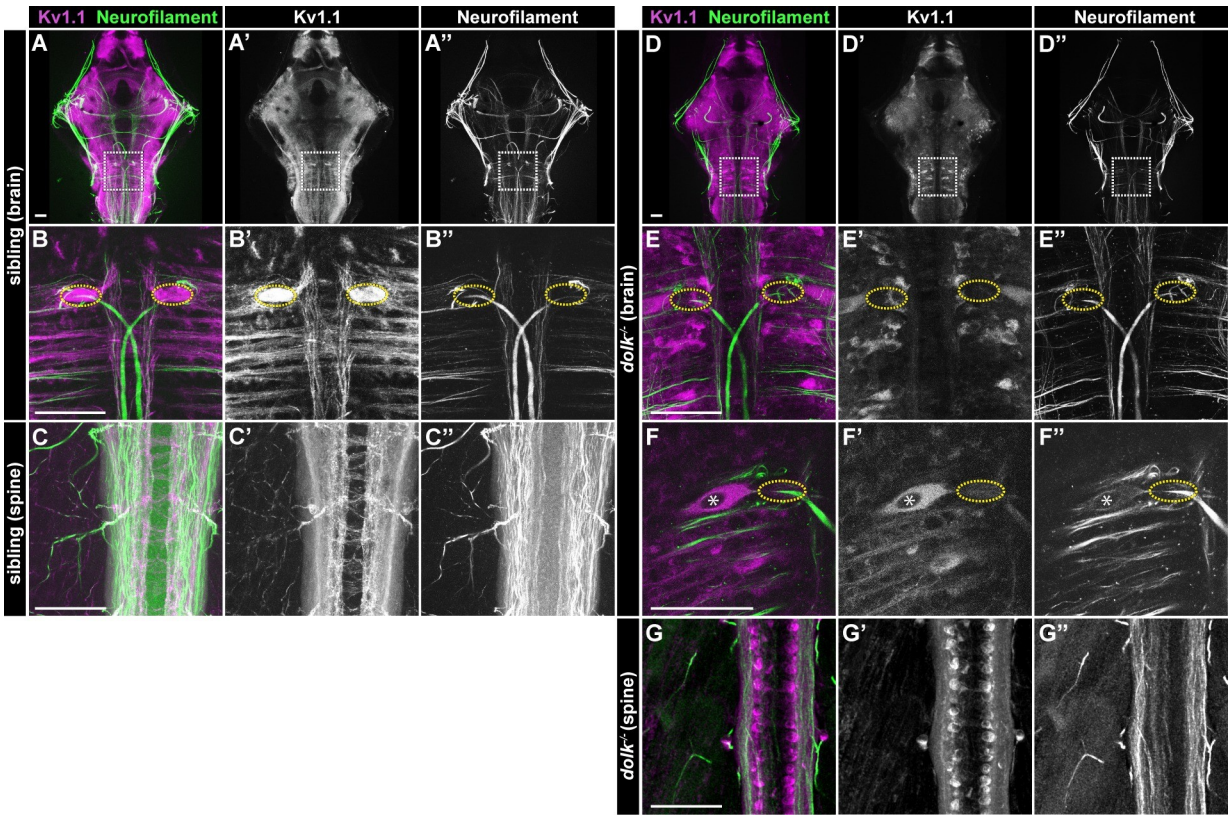

Fig 4. Dolk is required for proper localization of Kv1.1. (A-C) In 5 dpf *dolk* sibling larvae, Kv1.1 (magenta:A,B,C; grey:A',B',C') localizes to fiber tracts (α-3A10 antibody stains neurofilament; green:A,B,C; grey:A",B",C") throughout the brain (A; box indicates hindbrain zoom in B) and spinal cord (C). Particularly high accumulation of Kv1.1 is observed at the axon cap (B, yellow dotted circle), where spiral fiber neurons form axo-axonic synapses with the Mauthner cell. (D-G) In *dolk* mutants, Kv1.1 is localized within somata of neurons throughout the brain and spinal cord and is strongly reduced along axons throughout the hindbrain (D,D',E,E'). Soma localization is particularly apparent in the large Mauthner neuron, and Kv1.1 is strikingly absent from its axon cap (F, nucleus marked by asterisk, E,F axon cap marked by dotted ovals). Scale bars = 50 μM.

https://doi.org/10.1371/journal.pgen.1008943.g004

Mauthner cell acquiring single spike properties [55,56]. Furthermore, inhibition of Kv1 channels by local bath application of dendrotoxin-I onto the Mauthner cell lowers the threshold required to induce multiple spikes in the Mauthner cell [55,56]. Based on these previous findings, it is possible that *kcna1a* functions in Mauthner neurons to regulate the magnitude of the startle response. We explored this possibility using whole-cell recordings to determine the electrophysiological properties of Mauthner cells in sibling and *kcna1a* mutant larvae. Averaged measurements of membrane resting potential ($V_{resting}$), input resistance (R_{in}), rheobase (amount of current necessary to trigger an action potential), and action potential threshold ($V_{threshold}$) are not significantly different between siblings and *kcna1a* mutant larvae (S2A Fig). Next, we asked whether loss of *kcna1a* function changes the weight of key synaptic inputs to the Mauthner cells. Auditory afferents known as "large myelinated club endings" (club endings) that terminate on the lateral dendrite of the Mauthner cell are critical inputs for the acoustic startle response [57,58]. To test whether this synaptic input was altered, we examined mixed (electrical and chemical) synaptic potentials evoked by electrical stimulation of club endings in sibling and *kcna1a* mutant larvae during whole-cell recordings on the Mauthner cell (S2B Fig). We observed no difference in the average amplitudes of either the electrical (S2C Fig) or chemical (S2D Fig) components of the mixed synaptic response, nor in the

paired-pulse ratio of the chemical component (S2E Fig) indicating no changes in presynaptic neurotransmitter release. Finally, we failed to detect any significant difference in the half-width action potential between siblings and *kcna1a* mutants. Combined, these results reveal that neither changes of the excitability of Mauthner cells nor changes in the weight of critical auditory synaptic inputs can explain the exaggerated startle behavior observed in *kcna1a* mutants.

While Mauthner cell function and club endings appear unaffected in *kcna1a* mutants, it is possible that other inputs onto the Mauthner cells or synapses of the Mauthner cells are disrupted in *kcna1a* mutants. To determine whether *kcna1a* acts in a Mauthner-dependent pathway, we ablated Mauthner cells in *kcna1a* mutant larvae. Following Mauthner cell ablation, wild type larvae presented with an acoustic stimulus perform a longer latency, Mauthner-independent turning maneuver [16]. Thus, analyzing behavior in *kcna1a* mutants in which Mauthner neurons are ablated can clarify whether the exaggerated phenotype is dependent on Mauthner cell function and/or the function of neurons 'upstream' of Mauthner cells. We chemogenetically ablated Mauthners in *kcna1a* siblings and mutants using the nitroreductase (NTR)/metronidazole (Mtz) system [59]. Specifically, we utilized *62a*:*Gal4* [60] to drive Mauthner expression of *UAS*:*NTR-RFP*. With this genotype, expression was mosaic, so that some *62a*:*Gal4*, *UAS*:*NTR-RFP* larvae had expression in both Mauthner neurons, some in only one Mauthner neuron, and some in neither Mauthner neuron. This mosaicism allowed us to compare identical genotypes for ablation in larvae with initial Mauthner expression of NTR-RFP and without expression of NTR-RFP. Prior to Mtz treatment, larvae were scored for presence or absence of Mauthner cell NTR-RFP expression (Fig 5A and 5B). Following Mtz treatment, in larvae initially lacking Mauthner NTR-RFP expression, Mauthner neurons were intact (Fig 5C). Conversely, following Mtz treatment in larvae with initial Mauthner NTR-RFP expression, Mauthner neurons were undetectable (Fig 5D). We then presented fish with intact (controls) or ablated Mauthner cells with an acoustic stimulus. As expected, compared to controls, sibling and *kcna1a* mutant larvae in which Mauthner cells were ablated display a longer latency response characteristic of Mauthner-independent turning maneuvers (Fig 5E) [16]. Importantly, *kcna1a* mutant larvae in which Mauthner cells were ablated still performed exaggerated responses and figure eight turns (Fig 5F–5H). These responses were, aside from latency, indistinguishable from responses in mutants with intact Mauthner cells (S5 Video). Thus, the exaggerated behavioral response in *kcna1a* mutants is independent of activity in neurons 'upstream' of the Mauthner cell or in the Mauthner cell itself, further supporting the notion that Dolk and Kv1.1 primarily act outside the Mauthner-dependent hindbrain startle circuit to regulate startle magnitude.

We next tested whether *dolk* and *kcna1a* act in the spinal cord to regulate startle magnitude. We first determined whether *dolk* and *kcna1a* mutants exhibit any abnormal swim movements in the absence of external stimuli. *kcna1a* mutants execute normal swimming behaviors, including slow scoots and turns (Fig 6A and 6B) and when compared with their siblings, initiate a similar number of spontaneous movements (Fig 6G). However, after *kcna1a* mutant larvae begin a scoot maneuver, they sometimes undergo a series of rapid, high amplitude turns, similar to the behavior observed in response to acoustic stimuli (Fig 6C and S6 Video). This exaggerated "thrashing" movement is not observed in *kcna1a* siblings (n = 17 larvae, >800 responses), while *kcna1a* mutant larvae exhibit this behavior 22% of the time during spontaneous swim movements (Fig 6H). *dolk* mutant larvae also display exaggerated spontaneous swim movements (Fig 6H; 76% of spontaneous movements). Additionally, compared to siblings, *dolk* mutants initiate fewer spontaneous movements (Fig 6G), though each swim bout tends to be much longer (sibling average distance per swim bout = 10.9 a.u., mutant average distance

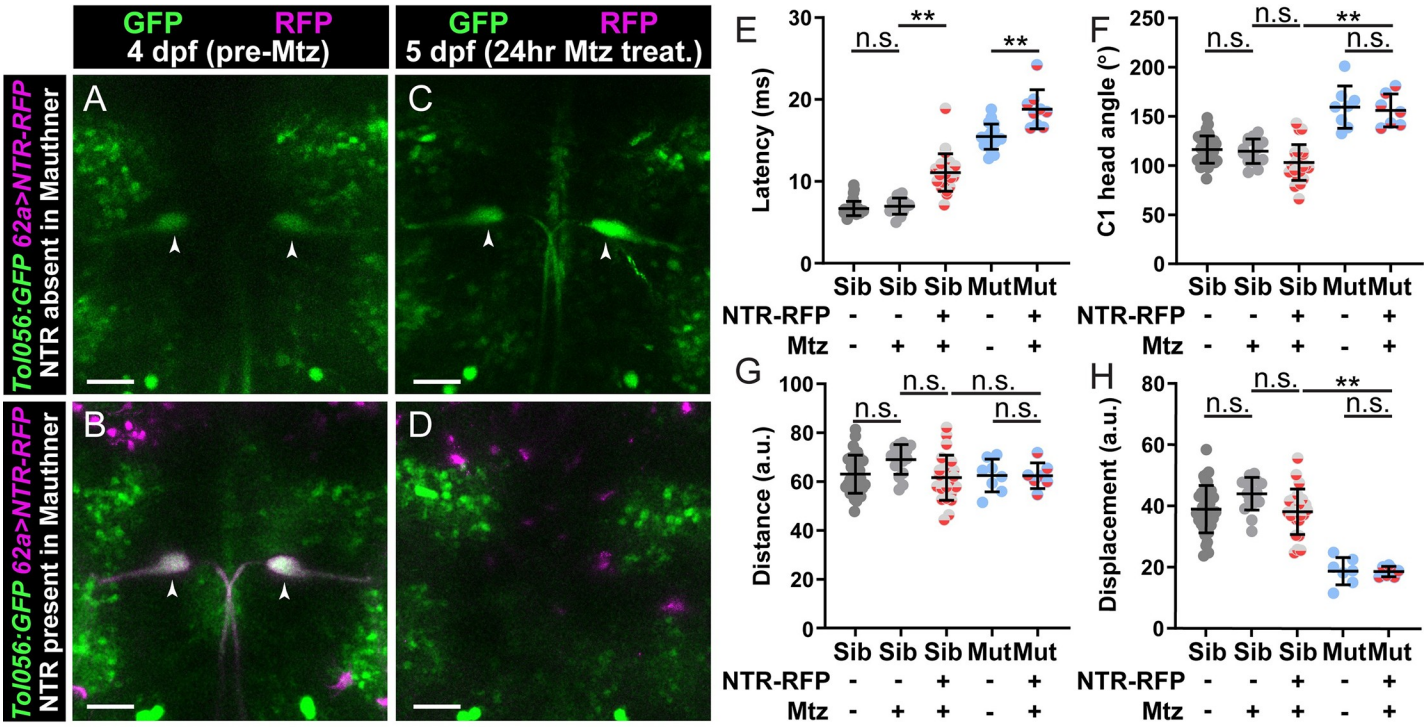

Fig 5. Kv1.1 functions outside the Mauthner command neuron to control swim movement magnitude. (A-D) *kcna1a* mutants expressing *Tol056* (GFP in Mauthner cells; green), *62a:Gal4* (Mauthner specific) and *UAS:NTR-RFP* (magenta). 62a>NTR-RFP is mosaic so some fish do not display expression in Mauthner cells (A) while others do (B). Before treatment with metronidazole (Mtz) at 4 dpf, all fish have GFP+ Mauthner cells (A,B). After 24 hr Mtz treatment, Mauthner cells are present in fish without initial NTR-RFP Mauthner expression (C) and absent in fish that displayed initial Mauthner NTR-RFP expression (D). (E-H) Kinematic parameters of the acoustic startle response in *kcna1a* sibling and mutant larvae with or without NTR-RFP expression in Mauthners and with or without Mtz treatment. Each point is the average response over ten trials for an individual larva. n≥9 larvae, **p<0.0001 (one-way ANOVA with Tukey correction for multiple comparisons). Scale bars = 50 μM.

https://doi.org/10.1371/journal.pgen.1008943.g005

per swim bout = 65.0 a.u.). Thus, *kcna1a* and *dolk* regulate the magnitude of both acoustic startle responses and spontaneous swim movements.

To address whether Dolk and Kv1.1 act primarily in spinal circuits to drive movement, we removed brain input to the body by severing the spinal cord. Zebrafish larvae can be "spinalized" by severing the head from the trunk and leaving only the spine intact. These spinalized larvae are unable to perform acoustic startle responses but are still capable of initiating spontaneous movement [61], though the rate of movement is reduced. We therefore transected the spinal cords of sibling and *dolk*/*kcna1a* mutant larvae (Fig 6D) and observed their spontaneous movement. Compared to intact *kcna1a* mutant larvae, spinalized *kcna1a* mutant larvae continue to exhibit exaggerated swim bouts not observed in spinalized siblings (Fig 6E–6H and S7 Video). Spinalized *dolk* mutant larvae also continue to exhibit exaggerated swim bouts (Fig 6H). Combined, these results demonstrate that Dolk and Kv1.1 are required in spinal locomotor circuits to control swim movement magnitude.

Finally, we asked in which motor circuits Dolk and Kv1.1 act to control swim movements. Kv1 in *Drosophila* [62] and Kv1.1 in mice [63,64] play important roles in preventing overactivity of motor neurons. In zebrafish larvae, we observe expression of Kv1.1 in motor neuron axons (Fig 7A). These motor neurons innervate both fast and slow muscle. In wild type animals, slow motor circuits turn off as fast motor circuits are recruited during fast movement [47]. We predicted that if loss of *kcna1a* mutants causes hyperactivity in motor circuits, perhaps slow motor circuits remain engaged during the fast startle response, leading to

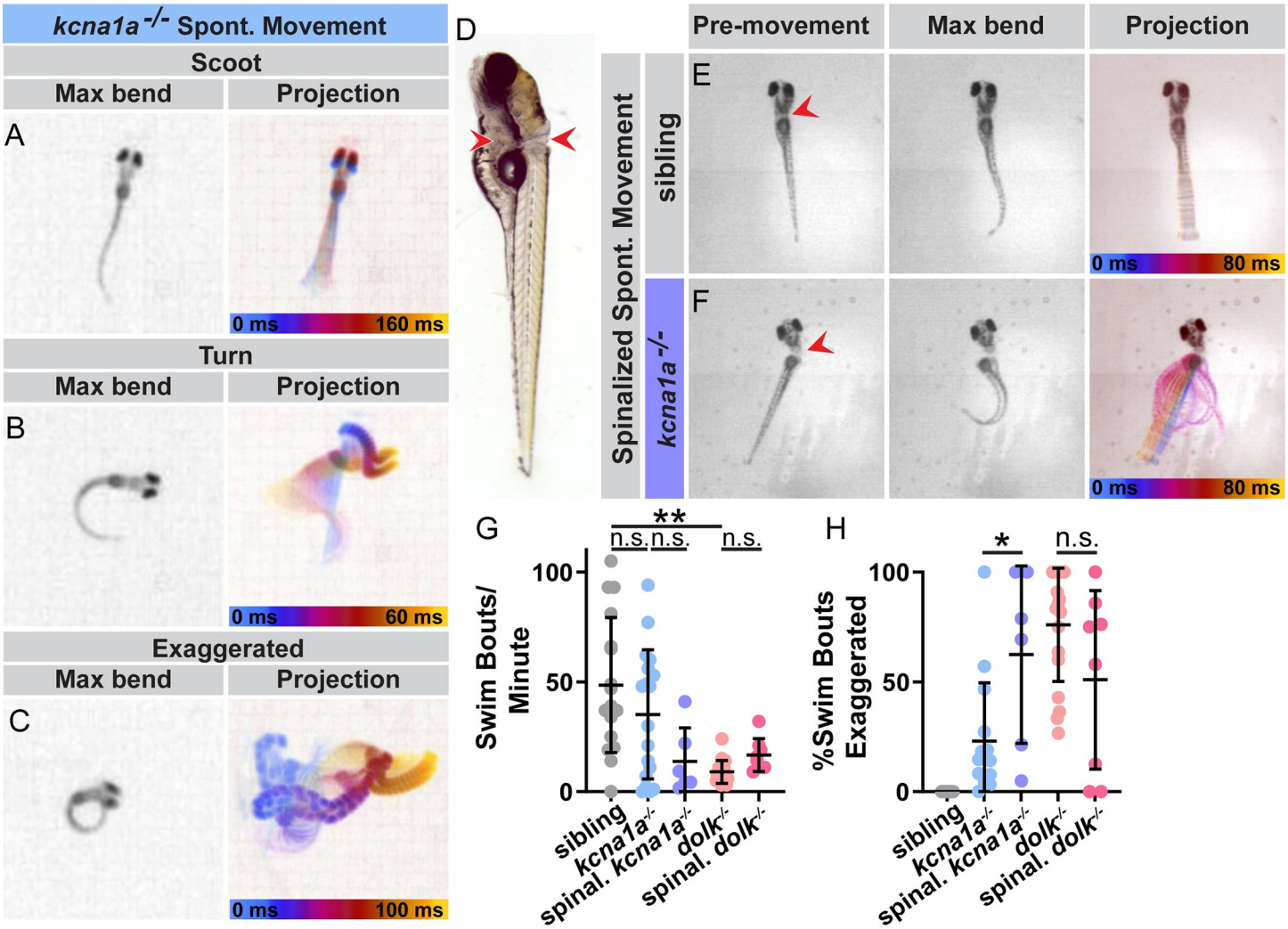

Fig 6. Kv1.1 and Dolk function in the spinal cord to control movement magnitude. (A-C) Examples of spontaneous swim movements performed by *kcna1a* mutant larvae. (D) Larvae were transected posterior to the brain to sever the spinal cord. Red arrows indicate the dorsal and ventral points of the cut. Some yolk was left intact to allow mounting of the head in agarose and imaging of the tails, which without the heads would lay on their sides. (E) Example of spinalized sibling and (F) spinalized *kcna1a* mutant spontaneous movement. (G) The number of spontaneous swim bouts initiated per minute for intact siblings and *kcna1a* mutants, spinalized *kcna1a* mutant larvae, intact *dolk* mutants, and spinalized *dolk* mutants (H) Percent of spontaneous swim bouts that are abnormal exaggerated movements with high amplitude bends. Each point is an individual fish. n≥6 fish. $^{**}p<0.0001$, $^{*}p = 0.0038$ (one-way ANOVA with Tukey correction for multiple comparisons).

https://doi.org/10.1371/journal.pgen.1008943.g006

overactivation of muscle contraction and the exaggerated turns observed in these mutant larvae. To test this idea, we generated double mutants in *dolk*, where Kv1.1 is drastically mislocalized in the spinal cord (Fig 4G), and *ryr1b*, which specifically disrupts fast muscle [33]. If slow motor circuits are hyperactive in *dolk* mutants, we would expect to see a rescue of the *ryr1b* behavioral phenotype in the double mutants. Instead, we observe *dolk*$^{-/-}$;*ryr1b*$^{-/-}$ mutant larvae display a very similar startle phenotype to *ryr1b* mutants. This indicates that Dolk, and likely also Kv1.1, primarily acts within fast motor circuits to regulate movement magnitude.

Fast locomotor circuits are comprised of fast motor neurons and both excitatory and inhibitory interneurons [47]. While it is possible *dolk* and *kcna1a* are solely required in motor neurons to drive correct movement magnitude, we observe Kv1.1 expressed broadly in the spinal cord, including in commissural axons and ipsilateral axon tracts (Fig 4C). Within fast motor

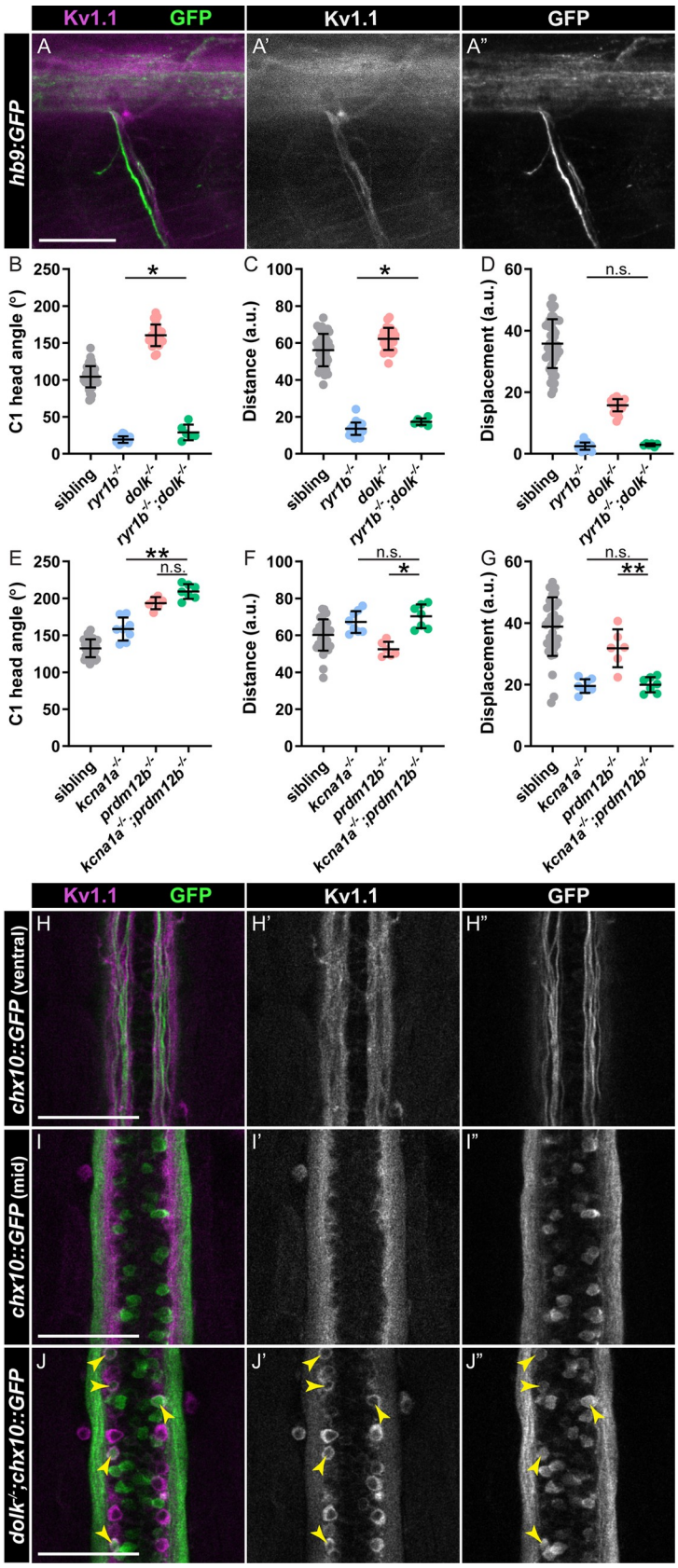
Kv1.1
GFP
Kv1.1
GFP
hb9:GFP
A
A'
A"
B
C1 head angle (°)
*
C
Distance (a.u.)
*
D
Displacement (a.u.)
n.s.
sibling
ryr1b-/-
dolk-/-
ryr1b-/-;dolk-/-
E
C1 head angle (°)
**
n.s.
F
Distance (a.u.)
n.s.
*
G
Displacement (a.u.)
n.s.
**
sibling
kcna1a-/-
prdm12b-/-
kcna1a-/-;prdm12b-/-
Kv1.1
GFP
Kv1.1
GFP
chx10::GFP (ventral)
H
H'
H"
chx10::GFP (mid)
I
I'
I"
dolk-/-;chx10::GFP
J
J'
J"

Fig 7. Kv1.1 is expressed in motor neurons and V2a interneurons. (A) Kv1.1 (magenta:A; grey:A') localizes to motor axons expressing hb9:GFP (green:A; grey:A"). (B-G) Kinematic parameters of the acoustic startle response in (B-D) sibling, *ryr1b* single mutants, *dolk* single mutants, and *ryr1b*$^{-/-}$;*dolk*$^{-/-}$ double mutants, and (E-G) sibling, *kcna1a* single mutants, *prdm12b* single mutants, and *kcna1a*$^{-/-}$;*prdm12b*$^{-/-}$ double mutants. Each point represents average of ten trials for an individual fish. n≥6 larvae, $^{*}p<0.04$ $^{**}p<0.0001$ (one-way ANOVA with Tukey correction for multiple comparisons). (H-I) Kv1.1 (magenta:H,I; grey:H',I') localizes to (H) V2a interneuron axons expressing chx10::GFP (green:H,I; grey:H",I") in the ventral spinal cord but not (I) V2a interneuron soma. (J) In *dolk* mutants, Kv1.1 (magenta:J; grey:J') localizes to V2a interneuron soma expressing chx10::GFP (green:J; grey:J"). Scale bars = 50 μM.

https://doi.org/10.1371/journal.pgen.1008943.g007

circuits, V1 inhibitory neurons ensure proper swim frequency during fast swim movements; ablation of these neurons [47] or loss through mutation of *prdm12b* ([45] and our results) results in reduced swim cycle frequency and prolonged bend duration. Based on Kv1.1's previous shown role in regulating neuron excitability [65–67], we predict loss of *kcna1a* induces hyperactivity in specific neurons, making it unlikely that loss of *kcna1a* in V1 neurons leads to the exaggerated response phenotype. However, it is possible that loss of *kcna1a* affects neurons upstream of V1 interneurons, leading to their inhibition. *prdm12b* and *kcna1a* mutants have similar but distinct acoustic startle phenotypes (Fig 7E–7G); while the initial turn angle is increased for both single mutants (Fig 7E), the "figure eight" movement, leading to reduced displacement (Fig 7G) is more pronounced in *kcna1a* mutants. We predicted that if *kcna1a* primarily acts upstream of V1 interneurons, *kcna1a/prdm12b* double mutants would display the *prdm12b* phenotype. Alternatively, if *kcna1a* acts primarily downstream or in parallel to V1 interneurons, double mutants would likely display the *kcna1a* phenotype. Double mutants display a strong exaggerated "figure eight" startle response, similar to *kcna1a* mutants (Fig 7E–7G). This suggests *kcna1a* may act in parallel or downstream to V1 interneurons, either solely in motor neurons, and/or in other interneurons.

One class of excitatory interneurons that act in combination with V1 interneurons to regulate fast locomotor circuits are the glutamatergic V2a Chx10+ interneurons. When V2a interneurons are silenced, the C1 turn angle and tail beat frequency following the acoustic stimulus are reduced [68]. V2a interneurons can be visualized in the spinal cord in *chx10*:*Gal4*, *UAS*:*GFP* (*chx10*::*GFP*) transgenic larvae (Fig 7H–7J"). Within the spinal cord where axons of V2a neurons project, we observe Kv1.1 protein localization (Fig 7H–7I"). To confirm Kv1.1 is expressed in V2a interneurons, we performed Kv1.1 staining in *dolk*$^{-/-}$;*chx10*::*GFP* larvae in which Kv1.1 is retained in the nucleus of cells throughout the spinal cord. We observed colocalization of Kv1.1 in a subset of GFP+ soma (Fig 7J). These results suggest that Kv1.1 may regulate movement magnitude through V2a interneurons.

Discussion

Movement initiation, magnitude, and duration all depend on neural circuits acting in a coordinated manner to drive muscle contraction. Here, we describe mutations in eight genes identified in a forward genetic screen in larval zebrafish that enable and ensure coordinated movements. The driving force for carrying out this screen was to discover, in an unbiased way, genes that are required to regulate the acoustic startle response. With this unbiased approach, we predicted we would identify both genes already implicated in locomotion and genes without a prior known role in locomotion. This is in fact what we found. All of the eight genes we identified in our screen are associated with human disorders, and six are associated with motor disorders (Table 1). For example, *NEB* mutations in humans are associated with nemaline myopathy, a congenital muscle disease characterized by muscle weakness [31]. We identified *neb* mutants based on their weak response to an acoustic stimulus, and a previously characterized zebrafish *neb* mutant was shown to have defects in sarcomere assembly [32],

similar to human patients with nemaline myopathy. Human mutations in *SLC5A7* are associated with congenital myasthenic syndrome [69], which is characterized by muscle weakness and fatigue. *slc5a7a* mutants from our screen display a weak acoustic startle response similar to *neb* mutants. While Neb protein acts within the muscle, Slc5a7 acts within motor neurons at the NMJ. Therefore, while the mutants have a similar phenotype, suggesting a similar site of action, the proteins act in different cell types. This underscores the importance of understanding the normal biological function of a protein when trying to understand the underlying cause of a genetic disorder.

Even when the function of a protein is known, the protein may act in many different neurons or cell types to regulate movement. For example, Kv1.1 is broadly expressed in the zebrafish nervous system ([55] and our work) and in the mammalian nervous system [54]. In humans, heterozygous disease alleles of the Kv1.1-encoding gene *KCNA1* have been shown to be causative for episodic ataxia (EA) Type 1 [70,71]. EA patients display frequent attacks of incoordination that are usually preceded by stress or startle. This phenotype is attributed to dysfunction in the cerebellum and peripheral nerves [72]. Work in mice heterozygous for a human *KCNA1* disease allele has demonstrated a cerebellar defect of action potential broadening in basket cells [73], and studies in patients with EA have demonstrated increased nerve excitability when the median nerve of the wrist was stimulated [67]. Thus, Kv1.1 acts at multiple points in the mammalian nervous system to regulate nerve activity.

In this study, we uncovered a brain-independent role for Kv1.1 in regulating swim movements in larval zebrafish. Spinalizing *kcna1a* mutant larvae fails to restore wild type motor function, suggesting that Kv1.1 plays a critical role in spinal motor circuits. Is Kv1.1 acting in interneurons, motor neurons, or both to drive movement? In zebrafish larvae, Kv1.1 is expressed throughout the spinal cord (Fig 4), including on axons of spinal motor neurons (Fig 7A). Kv1 plays an important role in regulating motor neuron activity across species. In *Drosophila*, there is a single Kv1 channel, Shaker, which was the first potassium channel ever cloned [74–76]. *Shaker* mutants exhibit aberrant movements and display broadened action potentials at NMJs [62]. In mice, Kv1.1 plays an important role in preventing spontaneous activity of motor neurons [63,64]. It is likely this role for Kv1.1 in motor neurons is conserved in zebrafish as well, though it is not yet clear to what extent this accounts for the behavioral defects in *kcna1a* mutants.

Another potential site of action for Kv1.1 in the spinal cord is in excitatory interneurons that activate motor neurons. One excitatory class is the V2a glutamatergic Chx10+ interneurons. In larval zebrafish, V2a interneurons are required for producing a normal acoustic startle response. When V2a interneurons are silenced, the C1 turn angle and tail beat frequency following the acoustic stimulus are reduced [68]. Recently, V2a interneurons in larval zebrafish have been categorized as Type I or Type II, similar to characterizations in mice, based on morphological and electrophysiological properties. From this work, type II V2a interneurons are predicted to regulate amplitude control [77]. We find that in the zebrafish spinal cord, Kv1.1 is expressed in a subset of V2a interneurons (Fig 7H–7J). It is therefore feasible that loss of Kv1.1 in type II V2a interneurons could result in hyperexcitability or broadening of the action potential, leading to increased recruitment or activation of motor neurons. This could explain the movement amplitude defects observed in *kcna1a* mutant larvae. Classes of locomotor interneurons are mostly conserved between fish and mammals [78], and single nucleus RNA-seq performed in mouse spinal cord neurons has revealed that *Kcna1* is enriched in V2a interneurons [79]. Moreover, in mice, V2a interneurons are critical to coordinate left-right alternating movement, particularly at high speeds [80]. Kv1.1 may play a critical role in zebrafish in regulating locomotion through limiting excitability of V2a interneurons.

While expression in different neuronal cell types provides specificity to Kv1.1's function, post-translational modifications critically regulate Kv1.1 activity. We have previously shown that the palmitoyltransferase Hip14 palmitoylates Kv1.1, and both Hip14 and Kv1.1 are essential for zebrafish larvae to habituate to repeated acoustic stimuli [24]. Here, we demonstrate a role for a glycosylation pathway protein Dolk in regulating Kv1.1 localization. In cell culture, glycosylation of Kv1.1 is required for proper channel function [50–52]. Interestingly, in these studies, glycosylation appeared dispensable for channel localization to the cell membrane. Here, we find that in *dolk* mutants, where Kv1.1 is predicted to not be glycosylated, cell surface localization of Kv1.1 is drastically disrupted. This effect may be a direct consequence due to the lack of Kv1.1 glycosylation or may be an indirect effect caused by reduced glycosylation of trafficking proteins. For example, Leucine-rich glioma-inactivated 1 (LGI1) is a glycoprotein that promotes axonal localization of Kv1.1 in hippocampal cells [81]. Whether the effect is direct or indirect, loss of Dolk clearly drastically affects Kv1.1 cell surface localization, providing compelling in vivo evidence that Kv1.1 localization is dependent, directly or indirectly, on Dolk-dependent glycosylation.

How does loss of a ubiquitous protein cause nervous system specific defects? Protein glycosylation is required in all cell types, and Dolk is a critical part of the protein glycosylation pathway. *dolk* mRNA has been detected in all human tissues assayed, with the highest expression observed in the brain [82]. Patients with *dolk* disease alleles display a range of phenotypes. In some patients, homozygous loss of function mutations in *dolk* cause metabolic and heart defects that are often lethal early in life [82,83]. Patients with similar homozygous, loss of function *dolk* alleles have also been identified that at the time of diagnosis in childhood only present with neurological conditions, including seizures [84]. Recently, a *dolk* variant has been identified as a potential risk gene in a patient with autism spectrum disorder [85]. The neurological symptoms observed in patients with *dolk* mutations underscore the importance of protein glycosylation in the nervous system [86]. In fact, defects in the nervous system are a predominant feature of congenital disorders of glycosylation [87]. Zebrafish *dolk* mutants do not display obvious morphological defects by 5 dpf except for failure to inflate their swim bladders, which is common in mutants with swim defects [11]. Homozygous *dolk* mutants die by 14 dpf, although we have not investigated the precise cause for this lethality. Lethality could be due to a failure to feed as zebrafish larvae must perform coordinated swim movements for prey hunting and feeding. Lethality could also be due to a broader requirement of *dolk* in vital organ systems.

In contrast, the behavioral phenotype in *dolk* mutants is highly specific and fairly unique. While Kv1.1 is likely not the only disrupted protein in *dolk* mutants, the similarity in behavioral phenotypes of *kcna1a* and *dolk* mutants suggests Kv1.1 is a critical protein affected by loss of *dolk*. It would be interesting to investigate whether similar dysregulation of Kv1.1 occurs in patients with neurological phenotypes arising from *dolk* mutations.

Together, this work demonstrates the utility of zebrafish for understanding genetic mechanisms driving regulation of locomotion. While the neural circuits driving movement are not identical among species, many of the genes required for circuit development and function are conserved. This is especially apparent from the number of genes identified from our screen that are associated with locomotor disorders in humans. In addition, while startle behaviors differ between species, the behavioral phenotypes associated with gene mutations are in some instances remarkably similar. For example, mice with *kcna1* mutations are hypersensitive to acoustic stimuli, display increased response latency during the acoustic startle response, and demonstrate increased amplitude of the response [88], similar to the acoustic startle phenotypes we observe in *kcna1a* mutant zebrafish larvae ([23] and this study). Further understanding of how loss of critical genes affects locomotor behaviors will further shape our models of how molecular pathways act in behavioral circuits to drive movement.

Methods

Ethics statement

All animal protocols were approved by the University of Pennsylvania Institutional Animal Care and Use Committee (IACUC).

Zebrafish husbandry and lines

Embryos were raised at 29˚C on a 14-h:10-h light:dark cycle in E3 media. *Tol056* is from [22]. *hspGFF62A* (*62a*,*Gal4*) is from [60]. *UAS:NTR-RFP* is from [89]. *chx10*:*Gal4* is from [90].

Behavior testing

Behavioral experiments were performed using 5 dpf larvae (except for Mauthner ablation experiments performed at 6 dpf) and analyzed using FLOTE software as described previously [16]. Larvae were tested in groups in a 6x6 laser cut grid. The acoustic stimuli used for acoustic startle experiments were 25.9 dB based on larval response rates and previous measurements of the speaker [25]. 10 stimuli were given with a 20 sec interstimulus interval. Before FLOTE tracking and analysis, ImageJ was used to remove background from videos to prevent erroneous measurements from the outline of the wells. Latency measurements in Table 1 were determined manually, as many mutants do not have swim bladders and lay on their sides and FLOTE did not always reliably calculate the movement latency. Angle measurements by FLOTE that were incorrect due to larvae laying on their sides and turning in the wrong plane were discarded. For measurements of spontaneous movement, only larvae that moved in a three-minute period were counted. Videos of acoustic startle response were acquired at 1000 fps, and videos of spontaneous movement were acquired at 125 fps. Images in figures have background removed, except for the spinalized larvae, and some images were mirrored to show an initial rightward turn for ease of comparison between genotypes.

Mutagenesis, WGS/WES, and transgenesis

ENU mutagenesis was performed using TLF and WIK as described previously [23]. Cloning of *p181* is described in [24].

Alleles *p415*, *p417*, and *p420* were cloned using WGS as described previously [25]. Alleles *p413*, *p414*, *p416*, and *p419* were cloned using WES as described previously [28]. For SNP analysis, we presumed our sibling pools (wild type behavior) consisted of 66% heterozygous (+/-) larvae and 33% (+/+) larvae, which results in a 1:2 ratio of mutant:wild type chromosomes in the analysis. To identify causative mutations and maintain mutant lines, mutations were genotyped using the following primers/reactions:

Gene^{allele}	Mutation (DNA, GRCz11)	Protocol	Primers
neb^{p413}	Chr 9:22844069 (C→A)	KASP	Sequences Proprietary–LGC Genomics
ryr1b^{p414}	Chr 18:35674009 (G→T)	KASP	Sequences Proprietary–LGC Genomics
cacna1ab^{p415}	Chr 11:30912033 (C→A)	KASP	Sequences Proprietary–LGC Genomics
rapsn^{p416}	Chr 18:20494662 (A→T)	PCR+ seq.	TGGGTCAGGACCAAACCAAA/GGCCGAGTTTGTCCATATGTT
slc5a7a^{p417}	Chr 1:34251722 (G→A)	KASP	Sequences Proprietary–LGC Genomics
prdm12b^{p419}	Chr 5:63511834 (T→C)	DCAPS+ AgeI	GAGACCTCATAAAGGCTCGAAA/GTGTTGTGGGAATTCCCATACCACACAACC
dolk^{p420}	Chr 21:4535709 (G→A)	KASP	Sequences Proprietary–LGC Genomics
dolk^{p421}	Chr 21:4535753 (G del.)	PCR+ seq.	TGGCTGTATGTGAGAGGACA/CGCTCCATGTAGACGTTTCC
kcna1a^{p181}	Chr 25:19956347 (C→A)	KASP	Sequences Proprietary–LGC Genomics
kcna1a^{p410}	Chr 25:19956067 (CCTTTCA ins.)	KASP	Sequences Proprietary–LGC Genomics

https://doi.org/10.1371/journal.pgen.1008943.t002

To confirm the splice site mutation in *ryr1b*^{p414}, a forward primer was designed in exon 4 and a reverse primer was designed in exon 5. PCR performed on cDNA from *ryr1b* homozygous mutant larvae resulted in a larger product (245 bp), caused by retention of an intron, than the product from wild type larvae (153 bp).

To generate *dolk*^{p421}, a CRISPR-Cas9 Alt-R gRNA (IDT) was designed using CHOPCHOP [91]. gRNA was combined with Cas9 protein (PacBio) and injected into one-cell stage embryos. F1 progeny from injected embryos were screened for mutations by sequencing the region flanking the gRNA site and using the ICE Analysis tool (v2) (Synthego) to identify Cas9 induced indels. Mosaic injected carriers were outcrossed to establish stable lines.

Unless noted otherwise, homozygous mutants were identified by abnormal kinematic behavior and siblings (heterozygous carriers and wild type) were designated as larvae performing normal startle responses. All phenotypes described in the paper display 100% penetrance, based on sequencing of at least twenty larvae displaying the mutant phenotype and at least twenty larvae displaying the wild type phenotype in presumed siblings. We do not observe phenotypes in heterozygous carrier larvae in any of the mutants described. Unless otherwise noted, all mutant alleles discussed in the text are from the forward genetic screen.

To generate *Tg(hb9:slc5a7a,hb9:mKate)*^{p418}, *slc5a7a* was cloned from 5 dpf larval cDNA into PENTR-D-TOPO (Invitrogen). Gateway cloning was performed with a double *hb9* promoter pDest plasmid that includes I-SceI sites [92] to make *hb9:slc5a7a,hb9:mKate*. The construct and I-SceI were injected, as described previously [93], into one-cell stage embryos from an outcross of *slc5a7a*$^{p417/+}$. Successful integration was monitored by screening for mKate in the spinal cord. In S1 Fig, genotype was determined by screening for mKate expression and genotyping for *mKate* and *p417* mutation.

Immunohistochemistry

6–7 dpf larvae were sorted by behavioral phenotype. Larvae were fixed in 2% trichloroacetic acid (TCA) in 1xPBS for three hours. Larvae were washed with PBS-0.25% Triton, blocked in 2% Normal Goat Serum, 1% BSA, 1% DMSO in PBT, and incubated with 1/200 α-Kv1.1 (rabbit, Millipore AB5174) and 1/50 α-3A10 (mouse, Developmental Studies Hybridoma Bank) in block solution for two days at 4˚C. Following washes in PBT, larvae were incubated in secondary antibody overnight (1/400 anti-mouse 488, anti-rabbit 633; Millipore) at 4˚C. After washing, larvae were dehydrated progressively in 25%, 50%, and 75% glycerol in PBS. Larvae were peeled to separate the spinal cord and brain and mounted ventral side towards the coverslip. Imaging was performed using a Zeiss LSM 880 confocal microscope.

Electrophysiology

To perform electrophysiological recordings from *kcna1a* siblings and mutants, larvae (5–8 dpf from an incross of *kcna1a*$^{p181/+}$*;Tol056*) were anesthetized using a 0.03% Tricaine solution pH adjusted to 7.4 with $NaHCO_3$. Larvae were then paralyzed using d-tubocurarine (10 μM, Sigma) in external solution in mM: 134 NaCl, 2.9 KCl, 2.1 $CaCl_2$, 1.2 $MgCl_2$, 10 HEPES, 10 Glucose, pH adjusted to 7.8 with NaOH [49]. Then, larvae were transferred dorsal-side down to a Sylgard-coated small culture dish (FluoroDish, WPI) and immobilized with tungsten pins. The brain was exposed ventrally as described in [17]. Following surgery, the petri dish containing the larva was placed on the stage of an Axio Examiner upright microscope (Carl Zeiss AG) adapted for electrophysiology recordings. Larvae were superfused with external solution throughout the recording session. Mauthner cells were identified by far-red DIC optics and GFP fluorescence. The patch pipette (3–4 MΩ) was filled with internal solution in mM: 105 K-Methanesulfonate, 10 HEPES, 10 EGTA, 2 $MgCl_2$, 2 $CaCl_2$, 4 Na_2ATP, 0.4 Tris-GTP, 10 K_2-

Phosphocreatine, 25 mannitol, pH adjusted to 7.2 with KOH. Whole-cell recordings under current-clamp configuration were performed using a Multiclamp 700B patch-clamp amplifier connected to a Digidata 1440A (Molecular Devices) digitizer. The liquid junction potential was estimated in -16 mV using Clampex 10.6 (Molecular Devices). The rheobase, defined as the minimum amount of positive current needed to elicit an action potential, was determined by delivering a 20 ms current pulse. Voltage threshold was measured as the membrane potential value at which the depolarizing-current step elicits an action potential. The input resistance was estimated using the voltage deflection caused by a hyperpolarizing-current step of -1 nA and 20 ms duration, followed by derivation of resistance with Ohm's law. To activate the auditory afferents to the Mauthner cell, a "theta" septated glass pipette filled with external solution was used as bipolar electrode. The bipolar electrode was placed at the posterior macula of the ear, where the dendritic processes of auditory afferents contact the hair cells [58].

Mauthner cell ablation

Larvae (obtained from a cross of *kcna1a*^{p181}/+;*Tol056*/+;*UAS*:*NTR-RFP*/+ and *kcna1a*^{p181}/+;*62a*:*Gal4*/+) were sorted at 60 hpf for GFP+ (*Tol056*) and NTR-RFP+ on a fluorescent dissecting scope. At 4 dpf, larvae were behavior tested and sorted into mutants and siblings. Because *62a>NTR-RFP* is mosaic, larvae expressing NTR-RFP in the brain were then mounted in agarose and screened on a compound epifluorescent scope for specific expression of NTR-RFP+ in the Mauthner cells. Only fish where both or neither Mauthner cells displayed expression were used. At 104 hpf, larvae were treated with 10mM Metronidazole/Mtz (Sigma-Aldrich) in 0.2% DMSO in E3. After 24 hours, Mtz was washed out and larvae were mounted and screened again to confirm ablation. At 144 hpf, larvae were behavior tested. Representative images of live fish in Fig 5 were obtained from a Zeiss LSM 880 confocal microscope.

Larvae spinalization

5 dpf larvae were anesthetized with Tricaine (Sigma-Aldrich) in Hank's balanced salt solution supplemented with 1x Glutamax and 1x sodium pyruvate. A sliver from a double edge razor was used to cut through the spinal cord and musculature through into the yolk, posterior to the brain, roughly at the halfway point of the swim bladder. Larvae were mounted in 2% low melt agarose in supplemented Hank's and agarose covering the tail was removed. Larvae were allowed to recover 30 min-2 hours in Hank's solution without Tricaine, until spontaneous movement was observed.

Statistics

Statistical analyses were performed using GraphPad Prism (tests used are listed in figure legends). All plots display mean and standard deviation.

Supporting information

S1 Data. Raw data numbers for all graphs.
(XLSX)

S1 Fig. The high affinity choline transporter Slc5a7a is required in motor neurons for the startle response. (A) Gene structure for *slc5a7a*, with the nonsense mutation from the screen (allele *p417*) noted. (B) Protein structure for Slc5a7a on the plasma membrane, with the predicted amino acid change from the screen mutation indicated. In contrast to siblings (C-G), *slc5a7a* mutants (H-L) display a weak startle response, with reduced bend and counter bend angles, as well as uncoordinated movement. Blue bar = latency in G,L. (M) *slc5a7a-/-; Tg(hb9;*

slc5a7a, *hb9:mKate)* larvae express mKate and *slc5a7a* in motor neurons. mKate is expressed from a second *hb9* promoter to allow visualization of expressing neurons without disrupting protein function. Bracket indicates motor column and arrow indicates motor nerve axons. Scale bar = 50 μM. (N-P) Kinematic parameters of the acoustic startle response in *slc5a7a* siblings and mutants with or without *hb9:slc5a7a* transgene. Each point represents an average of ten trials for an individual fish. $n \geq 15$ larvae, $^{*}p = 0.002$, $^{**}p < 0.0001$ (one-way ANOVA with Tukey correction for multiple comparisons).
(TIF)

S2 Fig. Electrophysiological properties of the Mauthner cell are unaffected in *kcna1a* mutant larvae. (A) Averaged measurements of $V_{resting}$, $V_{threshold}$, Rheobase, and R_{in} in *kcna1a* sibling and mutant larvae. n.s. = not significant. (B) Representative mixed synaptic responses on the Mauthner cell evoked by electrical stimulation of auditory afferents (club endings) in *kcna1a* sibling (left) and mutant (right) larvae (responses represent the average of at least 10 single traces). The maximal amplitude of the electrical component (C), chemical component (D), paired-pulse ratio of the chemical component (E), and half width AP (F) of the mixed synaptic response in *kcna1a* sibling or mutant Mauthner cells are not significantly different. n = 7 *kcna1a* sibling larvae, n = 6 (C-E)/5 (F) *kcna1a* mutant larvae. Mann-Whitney tests used for p-values.
(TIF)

S1 Video. Acoustic startle response of 5 dpf wild type larva. Stimulus is given at the start of the video and 90 ms of the response are shown. Video is slowed down 50x.
(MP4)

S2 Video. Acoustic startle response of 5 dpf *ryr1b* mutant larva. Stimulus is given at the start of the video and 90 ms of the response are shown. Video is slowed down 50x.
(MP4)

S3 Video. Acoustic startle response of 5 dpf *prdm12b* mutant larva. Stimulus is given at the start of the video and 90 ms of the response are shown. Video is slowed down 50x.
(MP4)

S4 Video. Acoustic startle response of 5 dpf *slc5a7a* mutant larva. Stimulus is given at the start of the video and 90 ms of the response are shown. Video is slowed down 50x.
(MP4)

S5 Video. Acoustic startle responses of 6 dpf *kcna1a* mutant larvae with or without intact Mauthner neurons. Larva with intact Mauthner neurons is on the left, and larva with ablated Mauthner neurons is on the right. Stimulus is given at the start of the video and 90 ms of the response are shown. Video is slowed down 50x.
(MP4)

S6 Video. Examples of spontaneous movements by a *kcna1a* mutant larva. Example of normal scoot, normal turn, and abnormal exaggerated movement are shown. Time labels refer to each individual movement type. Video is slowed down 50x.
(MP4)

S7 Video. Abnormal movements of a spinalized *kcna1a* mutant larva. Larva has had the spinal cord severed and the head is mounted in agarose. Two examples of spontaneous abnormal exaggerated movements are shown. Time labels refer to each individual movement type. Video is slowed down 50x.
(MP4)

Acknowledgments

The authors would like to thank Mary Mullins, Shannon Fisher, Bill Vought, Paula Roy, Hannah Bell, and Julianne Skinner for help with the genetic screen; Harold Burgess for *UAS:NTR-RFP*; the UPenn Cell & Developmental Biology Microscopy Core, UPenn Next-Generation Sequencing Core (WGS), and Duke Sequencing and Genomic Technologies Shared Resource (WES) for equipment and sequencing; Katharina Hayer for design of WGS pipeline; and members of the Granato lab for feedback regarding the manuscript.

Author Contributions

Conceptualization: Joy H. Meserve, Kurt C. Marsden, Roshan A. Jain, Marc A. Wolman, Michael Granato.

Data curation: Joy H. Meserve, Jessica C. Nelson, Kurt C. Marsden, Jerry Hsu.

Formal analysis: Joy H. Meserve, Jessica C. Nelson, Kurt C. Marsden, Jerry Hsu, Fabio A. Echeverry.

Funding acquisition: Joy H. Meserve, Alberto E. Pereda, Michael Granato.

Investigation: Joy H. Meserve, Jessica C. Nelson, Kurt C. Marsden, Jerry Hsu, Fabio A. Echeverry, Roshan A. Jain, Marc A. Wolman.

Methodology: Joy H. Meserve, Jessica C. Nelson, Kurt C. Marsden, Fabio A. Echeverry, Roshan A. Jain, Marc A. Wolman, Alberto E. Pereda, Michael Granato.

Project administration: Joy H. Meserve, Michael Granato.

Supervision: Michael Granato.

Visualization: Joy H. Meserve.

Writing – original draft: Joy H. Meserve.

Writing – review & editing: Joy H. Meserve, Fabio A. Echeverry, Alberto E. Pereda, Michael Granato.

References

1. Meincke U, Light GA, Geyer MA, Braff DL, Gouzoulis-Mayfrank E. Sensitization and habituation of the acoustic startle reflex in patients with schizophrenia. Psychiatry Res. 2004 Apr; 126(1):51–61. https://doi.org/10.1016/j.psychres.2004.01.003 PMID: 15081627
2. Takahashi H, Nakahachi T, Komatsu S, Ogino K, Iida Y, Kamio Y. Hyperreactivity to weak acoustic stimuli and prolonged acoustic startle latency in children with autism spectrum disorders. Mol Autism. 2014; 5(1):23. https://doi.org/10.1186/2040-2392-5-23 PMID: 24618368
3. Naegeli C, Zeffiro T, Piccirelli M, Jaillard A, Weilenmann A, Hassanpour K, et al. Locus Coeruleus Activity Mediates Hyperresponsiveness in Posttraumatic Stress Disorder. Biol Psychiatry. 2018 Feb; 83 (3):254–62. https://doi.org/10.1016/j.biopsych.2017.08.021 PMID: 29100627
4. Braff DL, Geyer MA, Swerdlow NR. Human studies of prepulse inhibition of startle: normal subjects, patient groups, and pharmacological studies. Psychopharmacology (Berl). 2001 Jul; 156(2–3):234–58. PMID: 11549226
5. Fetcho JR, McLean DL. Startle response. Encyclopedia of Neuroscience. 2009;375–9. https://doi.org/10.1016/B978-008045046-9.01973-2
6. Eaton RC, Bombardieri RA, Meyer DL. The Mauthner-initiated startle response in teleost fish. J Exp Biol. 1977; 66:65–81. PMID: 870603
7. Davis M, Gendelman D, Tischler M, Gendelman P. A primary acoustic startle circuit: lesion and stimulation studies. J Neurosci. 1982 Jun 1; 2(6):791–805. https://doi.org/10.1523/JNEUROSCI.02-06-00791.1982 PMID: 7086484

8. Lee Y, López DE, Meloni EG, Davis M. A Primary Acoustic Startle Pathway: Obligatory Role of Cochlear Root Neurons and the Nucleus Reticularis Pontis Caudalis. J Neurosci. 1996 Jun 1; 16(11):3775–89. https://doi.org/10.1523/JNEUROSCI.16-11-03775.1996 PMID: 8642420

9. Hale ME, Katz HR, Peek MY, Fremont RT. Neural circuits that drive startle behavior, with a focus on the Mauthner cells and spiral fiber neurons of fishes. J Neurogenet. 2016 Apr 2; 30(2):89–100. https://doi.org/10.1080/01677063.2016.1182526 PMID: 27302612

10. Pissiota A, Frans Ö, Fredrikson M, Långström B, Flaten MA. The human startle reflex and pons activation: a regional cerebral blood flow study: Brain mechanisms in human startle. Eur J Neurosci. 2002 Jan; 15(2):395–8. https://doi.org/10.1046/j.0953-816x.2001.01870.x PMID: 11849306

11. Granato M, van Eeden FJ, Schach U, Trowe T, Brand M, et al. (1996) Genes controlling and mediating locomotion behavior of the zebrafish embryo and larva. Development. 1996; 123:399–413. PMID: 9007258

12. Hirata H, Saint-Amant L, Downes GB, Cui WW, Zhou W, Granato M, et al. Zebrafish bandoneon mutants display behavioral defects due to a mutation in the glycine receptor β-subunit. Proc Natl Acad Sci. 2005 Jun 7; 102(23):8345–50. https://doi.org/10.1073/pnas.0500862102 PMID: 15928085

13. Westerfield M, Liu DW, Kimmel CB, Walker C. Pathfinding and synapse formation in a zebrafish mutant lacking functional acetylcholine receptors. Neuron. 1990 Jun; 4(6):867–74. https://doi.org/10.1016/0896-6273(90)90139-7 PMID: 2361010

14. Muto A, Orger MB, Wehman AM, Smear MC, Kay JN, Page-McCaw PS, et al. Forward Genetic Analysis of Visual Behavior in Zebrafish. PLoS Genet. 2005 Nov 25; 1(5):e66. https://doi.org/10.1371/journal.pgen.0010066 PMID: 16311625

15. Chiu CN, Rihel J, Lee DA, Singh C, Mosser EA, Chen S, et al. A Zebrafish Genetic Screen Identifies Neuromedin U as a Regulator of Sleep/Wake States. Neuron. 2016 Feb; 89(4):842–56. https://doi.org/10.1016/j.neuron.2016.01.007 PMID: 26889812

16. Burgess HA, Granato M. Sensorimotor Gating in Larval Zebrafish. J Neurosci. 2007 May 2; 27 (18):4984–94. https://doi.org/10.1523/JNEUROSCI.0615-07.2007 PMID: 17475807

17. Koyama M, Kinkhabwala A, Satou C, Higashijima S, Fetcho J. Mapping a sensory-motor network onto a structural and functional ground plan in the hindbrain. Proc Natl Acad Sci. 2011 Jan 18; 108(3):1170–5. https://doi.org/10.1073/pnas.1012189108 PMID: 21199937

18. Tabor KM, Bergeron SA, Horstick EJ, Jordan DC, Aho V, Porkka-Heiskanen T, et al. Direct activation of the Mauthner cell by electric field pulses drives ultrarapid escape responses. J Neurophysiol. 2014 Aug 15; 112(4):834–44. https://doi.org/10.1152/jn.00228.2014 PMID: 24848468

19. Kohashi T, Oda Y. Initiation of Mauthner- or Non-Mauthner-Mediated Fast Escape Evoked by Different Modes of Sensory Input. J Neurosci. 2008 Oct 15; 28(42):10641–53. https://doi.org/10.1523/JNEUROSCI.1435-08.2008 PMID: 18923040

20. Ritter DA, Bhatt DH, Fetcho JR. In Vivo Imaging of Zebrafish Reveals Differences in the Spinal Networks for Escape and Swimming Movements. J Neurosci. 2001 Nov 15; 21(22):8956–65. https://doi.org/10.1523/JNEUROSCI.21-22-08956.2001 PMID: 11698606

21. Fetcho JR. Excitation of motoneurons by the Mauthner axon in goldfish: complexities in a "simple" reticulospinal pathway. J Neurophysiol. 1992 Jun 1; 67(6):1574–86. https://doi.org/10.1152/jn.1992.67.6.1574 PMID: 1629765

22. Satou C, Kimura Y, Kohashi T, Horikawa K, Takeda H, Oda Y, et al. Functional Role of a Specialized Class of Spinal Commissural Inhibitory Neurons during Fast Escapes in Zebrafish. J Neurosci. 2009 May 27; 29(21):6780–93. https://doi.org/10.1523/JNEUROSCI.0801-09.2009 PMID: 19474306

23. Wolman MA, Jain RA, Marsden KC, Bell H, Skinner J, Hayer KE, et al. A Genome-wide Screen Identifies PAPP-AA-Mediated IGFR Signaling as a Novel Regulator of Habituation Learning. Neuron. 2015 Mar; 85(6):1200–11. https://doi.org/10.1016/j.neuron.2015.02.025 PMID: 25754827

24. Nelson JC, Witze E, Ma Z, Ciocco F, Frerotte A, Randlett O, et al. Acute regulation of habituation learning via posttranslational palmitoylation. Curr Biol. 2020 Jul 20; 30(14):2729–38.e4. https://doi.org/10.1016/j.cub.2020.05.016 PMID: 32502414

25. Marsden KC, Jain RA, Wolman MA, Echeverry FA, Nelson JC, Hayer KE, et al. A Cyfip2-Dependent Excitatory Interneuron Pathway Establishes the Innate Startle Threshold. Cell Rep. 2018 Apr; 23 (3):878–87. https://doi.org/10.1016/j.celrep.2018.03.095 PMID: 29669291

26. Jain RA, Wolman MA, Marsden KC, Nelson JC, Shoenhard H, Echeverry FA, et al. A Forward Genetic Screen in Zebrafish Identifies the G-Protein-Coupled Receptor CaSR as a Modulator of Sensorimotor Decision Making. Curr Biol. 2018 May; 28(9):1357–69.e5. https://doi.org/10.1016/j.cub.2018.03.025 PMID: 29681477

27. Zannino DA, Downes GB, Sagerström CG. prdm12b specifies the p1 progenitor domain and reveals a role for V1 interneurons in swim movements. Dev Biol. 2014 Jun; 390(2):247–60. https://doi.org/10.1016/j.ydbio.2014.02.025 PMID: 24631215

28. Ryan S, Willer J, Marjoram L, Bagwell J, Mankiewicz J, Leshchiner I, et al. Rapid identification of kidney cyst mutations by whole exome sequencing in zebrafish. Development. 2013; 140(21):4445–51. https://doi.org/10.1242/dev.101170 PMID: 24130329

29. Leshchiner I, Alexa K, Kelsey P, Adzhubei I, Austin-Tse CA, Cooney JD, et al. Mutation mapping and identification by whole-genome sequencing. Genome Res. 2012; 22(8):1541–8. https://doi.org/10.1101/gr.135541.111 PMID: 22555591

30. Howe K, Clark MD, Torroja CF, Torrance J, Berthelot C, Muffato M, et al. The zebrafish reference genome sequence and its relationship to the human genome. Nature. 2013; 496(7446):498–503. https://doi.org/10.1038/nature12111 PMID: 23594743

31. Chu M, Gregorio CC, Pappas CT. Nebulin, a multi-functional giant. J Exp Biol. 2016; 219(Pt 2):146–52. https://doi.org/10.1242/jeb.126383 PMID: 26792324

32. Telfer WR, Nelson DD, Waugh T, Brooks SV, Dowling JJ. Neb: a zebrafish model of nemaline myopathy due to nebulin mutation. Dis Model Mech. 2012; 5(3):389–96. https://doi.org/10.1242/dmm.008631 PMID: 22159874

33. Hirata H, Watanabe T, Hatakeyama J, Sprague SM, Saint-Amant L, Nagashima A, et al. Zebrafish relatively relaxed mutants have a ryanodine receptor defect, show slow swimming and provide a model of multi-minicore disease. Development. 2007; 134(15):2771–81. https://doi.org/10.1242/dev.004531 PMID: 17596281

34. Svara FN, Kornfeld J, Denk W, Bollmann JH. Volume EM Reconstruction of Spinal Cord Reveals Wiring Specificity in Speed-Related Motor Circuits. Cell Rep. 2018; 23(10):2942–54. https://doi.org/10.1016/j.celrep.2018.05.023 PMID: 29874581

35. Menelaou E, McLean DL. A gradient in endogenous rhythmicity and oscillatory drive matches recruitment order in an axial motor pool. J Neurosci. 2012; 32(32):10925–39. https://doi.org/10.1523/JNEUROSCI.1809-12.2012 PMID: 22875927

36. Ono F, Shcherbatko A, Higashijima S, Mandel G, Brehm P. The Zebrafish motility mutant twitch once reveals new roles for rapsyn in synaptic function. J Neurosci. 2002; 22(15):6491–8. https://doi.org/10.1523/JNEUROSCI.22-15-06491.2002 PMID: 12151528

37. Low SE, Woods IG, Lachance M, Ryan J, Schier AF, Saint-Amant L. Touch responsiveness in zebrafish requires voltage-gated calcium channel 2.1b. J Neurophysiol. 2012; 108(1):148–59. https://doi.org/10.1152/jn.00839.2011 PMID: 22490555

38. Wen H, Linhoff MW, Hubbard JM, Nelson NR, Stensland D, Dallman J, et al. Zebrafish calls for reinterpretation for the roles of P/Q calcium channels in neuromuscular transmission. J Neurosci. 2013; 33(17):7384–92. https://doi.org/10.1523/JNEUROSCI.5839-12.2013 PMID: 23616544

39. Liu KS, Fetcho JR. Laser ablations reveal functional relationships of segmental hindbrain neurons in zebrafish. Neuron. 1999; 23(2):325–35. https://doi.org/10.1016/s0896-6273(00)80783-7 PMID: 10399938

40. Sarter M, Parikh V. Choline transporters, cholinergic transmission and cognition. Nat Rev Neurosci. 2005; 6(1):48–56. https://doi.org/10.1038/nrn1588 PMID: 15611726

41. Ono F, Higashijima S, Shcherbatko A, Fetcho JR, Brehm P. Paralytic zebrafish lacking acetylcholine receptors fail to localize rapsyn clusters to the synapse. J Neurosci. 2001; 21(15):5439–48. https://doi.org/10.1523/JNEUROSCI.21-15-05439.2001 PMID: 11466415

42. Flanagan-Steet H, Fox MA, Meyer D, Sanes JR. Neuromuscular synapses can form in vivo by incorporation of initially aneural postsynaptic specializations. Development. 2005; 132(20):4471–81. https://doi.org/10.1242/dev.02044 PMID: 16162647

43. Zannino DA, Sagerstrom CG. An emerging role for prdm family genes in dorsoventral patterning of the vertebrate nervous system. Neural Dev. 2015; 10:24. https://doi.org/10.1186/s13064-015-0052-8 PMID: 26499851

44. Choe SK, Zhang X, Hirsch N, Straubhaar J, Sagerstrom CG. A screen for hoxb1-regulated genes identifies ppp1r14al as a regulator of the rhombomere 4 Fgf-signaling center. Dev Biol. 2011; 358(2):356–67. https://doi.org/10.1016/j.ydbio.2011.05.676 PMID: 21787765

45. Yildiz O, Downes GB, Sagerstrom CG. Zebrafish prdm12b acts independently of nkx6.1 repression to promote eng1b expression in the neural tube p1 domain. Neural Dev. 2019; 14(1):5. https://doi.org/10.1186/s13064-019-0129-x PMID: 30813944

46. Gosgnach S, Lanuza GM, Butt SJ, Saueressig H, Zhang Y, Velasquez T, et al. V1 spinal neurons regulate the speed of vertebrate locomotor outputs. Nature. 2006; 440(7081):215–9. https://doi.org/10.1038/nature04545 PMID: 16525473

47. Kimura Y, Higashijima SI. Regulation of locomotor speed and selection of active sets of neurons by V1 neurons. Nat Commun. 2019; 10(1):2268. https://doi.org/10.1038/s41467-019-09871-x PMID: 31118414

48. Shridas P, Waechter CJ. Human dolichol kinase, a polytopic endoplasmic reticulum membrane protein with a cytoplasmically oriented CTP-binding site. J Biol Chem. 2006; 281(42):31696–704. https://doi.org/10.1016/S0021-9258(19)84083-8 PMID: 16923818

49. Baycin-Hizal D, Tian Y, Akan I, Jacobson E, Clark D, Wu A, et al. GlycoFish: a database of zebrafish N-linked glycoproteins identified using SPEG method coupled with LC/MS. Anal Chem. 2011; 83 (13):5296–303. https://doi.org/10.1021/ac200726q PMID: 21591763

50. Sutachan JJ, Watanabe I, Zhu J, Gottschalk A, Recio-Pinto E, Thornhill WB. Effects of Kv1.1 channel glycosylation on C-type inactivation and simulated action potentials. Brain Res. 2005; 1058(1–2):30–43. https://doi.org/10.1016/j.brainres.2005.07.050 PMID: 16153617

51. Watanabe I, Wang HG, Sutachan JJ, Zhu J, Recio-Pinto E, Thornhill WB. Glycosylation affects rat Kv1.1 potassium channel gating by a combined surface potential and cooperative subunit interaction mechanism. J Physiol. 2003; 550(Pt 1):51–66. https://doi.org/10.1113/jphysiol.2003.040337 PMID: 12879861

52. Thornhill WB, Wu MB, Jiang X, Wu X, Morgan PT, Margiotta JF. Expression of Kv1.1 delayed rectifier potassium channels in Lec mutant Chinese hamster ovary cell lines reveals a role for sialidation in channel function. J Biol Chem. 1996; 271(32):19093–8. https://doi.org/10.1074/jbc.271.32.19093 PMID: 8702582

53. Moremen KW, Tiemeyer M, Nairn AV. Vertebrate protein glycosylation: diversity, synthesis and function. Nat Rev Mol Cell Biol. 2012; 13(7):448–62. https://doi.org/10.1038/nrm3383 PMID: 22722607

54. Wang H, Kunkel DD, Schwartzkroin PA, Tempel BL. Localization of Kv1.1 and Kv1.2, 2 K-Channel Proteins, to Synaptic Terminals, Somata, and Dendrites in the Mouse-Brain. J Neurosci. 1994; 14(8):4588–99. https://doi.org/10.1523/JNEUROSCI.14-08-04588.1994 PMID: 8046438

55. Brewster DL, Ali DW. Expression of the voltage-gated potassium channel subunit Kv1.1 in embryonic zebrafish Mauthner cells. Neurosci Lett. 2013; 539:54–9. https://doi.org/10.1016/j.neulet.2013.01.042 PMID: 23384568

56. Watanabe T, Shimazaki T, Mishiro A, Suzuki T, Hirata H, Tanimoto M, et al. Coexpression of auxiliary Kvbeta2 subunits with Kv1.1 channels is required for developmental acquisition of unique firing properties of zebrafish Mauthner cells. J Neurophysiol. 2014; 111(6):1153–64. https://doi.org/10.1152/jn.00596.2013 PMID: 24335214

57. Zottoli SJ, Faber DS. Properties and distribution of anterior VIIIth nerve excitatory inputs to the goldfish Mauthner cell. Brain Res. 1979; 174(2):319–23. https://doi.org/10.1016/0006-8993(79)90854-0 PMID: 39661

58. Yao C, Vanderpool KG, Delfiner M, Eddy V, Lucaci AG, Soto-Riveros C, et al. Electrical synaptic transmission in developing zebrafish: properties and molecular composition of gap junctions at a central auditory synapse. Journal of Neurophysiology. 2014; 112(9):2102–13. https://doi.org/10.1152/jn.00397.2014 PMID: 25080573

59. Curado S, Stainier DY, Anderson RM. Nitroreductase-mediated cell/tissue ablation in zebrafish: a spatially and temporally controlled ablation method with applications in developmental and regeneration studies. Nat Protoc. 2008; 3(6):948–54. https://doi.org/10.1038/nprot.2008.58 PMID: 18536643

60. Kawakami K, Abe G, Asada T, Asakawa K, Fukuda R, Ito A, et al. zTrap: zebrafish gene trap and enhancer trap database. BMC Dev Biol. 2010; 10(105):105. https://doi.org/10.1186/1471-213X-10-105 PMID: 20950494

61. Downes GB, Granato M. Supraspinal input is dispensable to generate glycine-mediated locomotive behaviors in the zebrafish embryo. J Neurobiol. 2006; 66(5):437–51. https://doi.org/10.1002/neu.20226 PMID: 16470684

62. Mallart A, Angaut-Petit D, Bourret-Poulain C, Ferrus A. Nerve terminal excitability and neuromuscular transmission in T(X;Y)V7 and Shaker mutants of Drosophila melanogaster. J Neurogenet. 1991; 7(2–3):75–84. https://doi.org/10.3109/01677069109066212 PMID: 1851515

63. Brunetti O, Imbrici P, Botti FM, Pettorossi VE, D'Adamo MC, Valentino M, et al. Kv1.1 knock-in ataxic mice exhibit spontaneous myokymic activity exacerbated by fatigue, ischemia and low temperature. Neurobiol Dis. 2012; 47(3):310–21. https://doi.org/10.1016/j.nbd.2012.05.002 PMID: 22609489

64. Zhou L, Zhang CL, Messing A, Chiu SY. Temperature-sensitive neuromuscular transmission in Kv1.1 null mice: role of potassium channels under the myelin sheath in young nerves. J Neurosci. 1998; 18 (18):7200–15. https://doi.org/10.1523/JNEUROSCI.18-18-07200.1998 PMID: 9736643

65. Johnston J, Forsythe ID, Kopp-Scheinpflug C. Going native: voltage-gated potassium channels controlling neuronal excitability. J Physiol. 2010; 588(Pt 17):3187–200. https://doi.org/10.1113/jphysiol.2010.191973 PMID: 20519310

66. Goldberg EM, Clark BD, Zagha E, Nahmani M, Erisir A, Rudy B. K+ channels at the axon initial segment dampen near-threshold excitability of neocortical fast-spiking GABAergic interneurons. Neuron. 2008; 58(3):387–400. https://doi.org/10.1016/j.neuron.2008.03.003 PMID: 18466749

67. Tomlinson SE, Tan SV, Kullmann DM, Griggs RC, Burke D, Hanna MG, et al. Nerve excitability studies characterize Kv1.1 fast potassium channel dysfunction in patients with episodic ataxia type 1. Brain. 2010; 133(Pt 12):3530–40. https://doi.org/10.1093/brain/awq318 PMID: 21106501

68. Sternberg JR, Severi KE, Fidelin K, Gomez J, Ihara H, Alcheikh Y, et al. Optimization of a Neurotoxin to Investigate the Contribution of Excitatory Interneurons to Speed Modulation In Vivo. Curr Biol. 2016; 26 (17):2319–28. https://doi.org/10.1016/j.cub.2016.06.037 PMID: 27524486

69. Bauche S, O'Regan S, Azuma Y, Laffargue F, McMacken G, Sternberg D, et al. Impaired Presynaptic High-Affinity Choline Transporter Causes a Congenital Myasthenic Syndrome with Episodic Apnea. Am J Hum Genet. 2016; 99(3):753–61. https://doi.org/10.1016/j.ajhg.2016.06.033 PMID: 27569547

70. Browne DL, Gancher ST, Nutt JG, Brunt ER, Smith EA, Kramer P, et al. Episodic ataxia/myokymia syndrome is associated with point mutations in the human potassium channel gene, KCNA1. Nat Genet. 1994; 8(2):136–40. https://doi.org/10.1038/ng1094-136 PMID: 7842011

71. Glaudemans B, van der Wijst J, Scola RH, Lorenzoni PJ, Heister A, van der Kemp AW, et al. A missense mutation in the Kv1.1 voltage-gated potassium channel-encoding gene KCNA1 is linked to human autosomal dominant hypomagnesemia. J Clin Investig. 2009; 119(4):936–42. https://doi.org/10.1172/JCI36948 PMID: 19307729

72. Graves TD, Cha YH, Hahn AF, Barohn R, Salajegheh MK, Griggs RC, et al. Episodic ataxia type 1: clinical characterization, quality of life and genotype-phenotype correlation. Brain. 2014; 137(Pt 4):1009–18. https://doi.org/10.1093/brain/awu012 PMID: 24578548

73. Begum R, Bakiri Y, Volynski KE, Kullmann DM. Action potential broadening in a presynaptic channelopathy. Nat Commun. 2016; 7:12102. https://doi.org/10.1038/ncomms12102 PMID: 27381274

74. Kamb A, Iverson LE, Tanouye MA. Molecular characterization of Shaker, a Drosophila gene that encodes a potassium channel. Cell. 1987; 50(3):405–13. https://doi.org/10.1016/0092-8674(87)90494-6 PMID: 2440582

75. Timpe LC, Jan LY. Gene dosage and complementation analysis of the Shaker locus in Drosophila. J Neurosci. 1987; 7(5):1307–17. https://doi.org/10.1523/JNEUROSCI.07-05-01307.1987 PMID: 2437260

76. Baumann A, Krahjentgens I, Muller R, Mullerholtkamp F, Seidel R, Kecskemethy N, et al. Molecular Organization of the Maternal Effect Region of the Shaker Complex of Drosophila: Characterization of an Ia Channel Transcript with Homology to Vertebrate Na+ Channel. EMBO J. 1987; 6(11):3419–29. https://doi.org/10.1002/j.1460-2075.1987.tb02665.x PMID: 16453805

77. Menelaou E, McLean DL. Hierarchical control of locomotion by distinct types of spinal V2a interneurons in zebrafish. Nat Commun. 2019; 10(1):4197. https://doi.org/10.1038/s41467-019-12240-3 PMID: 31519892

78. Goulding M. Circuits controlling vertebrate locomotion: moving in a new direction. Nat Rev Neurosci. 2009; 10(7):507–18. https://doi.org/10.1038/nrn2608 PMID: 19543221

79. Sathyamurthy A, Johnson KR, Matson KJE, Dobrott CI, Li L, Ryba AR, et al. Massively Parallel Single Nucleus Transcriptional Profiling Defines Spinal Cord Neurons and Their Activity during Behavior. Cell Rep. 2018; 22(8):2216–25. https://doi.org/10.1016/j.celrep.2018.02.003 PMID: 29466745

80. Crone SA, Zhong G, Harris-Warrick R, Sharma K. In mice lacking V2a interneurons, gait depends on speed of locomotion. J Neurosci. 2009; 29(21):7098–109. https://doi.org/10.1523/JNEUROSCI.1206-09.2009 PMID: 19474336

81. Seagar M, Russier M, Caillard O, Maulet Y, Fronzaroli-Molinieres L, De San Feliciano M, et al. LGI1 tunes intrinsic excitability by regulating the density of axonal Kv1 channels. Proc Natl Acad Sci U S A. 2017; 114(29):7719–24. https://doi.org/10.1073/pnas.1618656114 PMID: 28673977

82. Lefeber DJ, de Brouwer AP, Morava E, Riemersma M, Schuurs-Hoeijmakers JH, Absmanner B, et al. Autosomal recessive dilated cardiomyopathy due to DOLK mutations results from abnormal dystroglycan O-mannosylation. PLoS Genet. 2011; 7(12):e1002427. https://doi.org/10.1371/journal.pgen.1002427 PMID: 22242004

83. Kranz C, Jungeblut C, Denecke J, Erlekotte A, Sohlbach C, Debus V, et al. A defect in dolichol phosphate biosynthesis causes a new inherited disorder with death in early infancy. Am J Hum Genet. 2007; 80(3):433–40. https://doi.org/10.1086/512130 PMID: 17273964

84. Helander A, Stodberg T, Jaeken J, Matthijs G, Eriksson M, Eggertsen G. Dolichol kinase deficiency (DOLK-CDG) with a purely neurological presentation caused by a novel mutation. Mol Genet Metab. 2013; 110(3):342–4. https://doi.org/10.1016/j.ymgme.2013.07.002 PMID: 23890587

85. Xiong J, Chen S, Pang N, Deng X, Yang L, He F, et al. Neurological Diseases With Autism Spectrum Disorder: Role of ASD Risk Genes. Front Neurosci. 2019; 13:349. https://doi.org/10.3389/fnins.2019.00349 PMID: 31031587

86. Scott H, Panin VM. The role of protein N-glycosylation in neural transmission. Glycobiology. 2014; 24 (5):407–17. https://doi.org/10.1093/glycob/cwu015 PMID: 24643084

87. Freeze HH, Eklund EA, Ng BG, Patterson MC. Neurology of inherited glycosylation disorders. The Lancet Neurology. 2012; 11(5):453–66. https://doi.org/10.1016/S1474-4422(12)70040-6 PMID: 22516080

88. Fisahn A, Lavebratt C, Canlon B. Acoustic startle hypersensitivity in Mceph mice and its effect on hippocampal excitability. Eur J Neurosci. 2011; 34(7):1121–30. https://doi.org/10.1111/j.1460-9568.2011.07834.x PMID: 21966978

89. Marquart GD, Tabor KM, Brown M, Strykowski JL, Varshney GK, LaFave MC, et al. A 3D Searchable Database of Transgenic Zebrafish Gal4 and Cre Lines for Functional Neuroanatomy Studies. Front Neural Circuits. 2015; 9:78. https://doi.org/10.3389/fncir.2015.00078 PMID: 26635538

90. Kimura Y, Satou C, Fujioka S, Shoji W, Umeda K, Ishizuka T, et al. Hindbrain V2a neurons in the excitation of spinal locomotor circuits during zebrafish swimming. Curr Biol. 2013; 23(10):843–9. https://doi.org/10.1016/j.cub.2013.03.066 PMID: 23623549

91. Labun K, Montague TG, Gagnon JA, Thyme SB, Valen E. CHOPCHOP v2: a web tool for the next generation of CRISPR genome engineering. Nucleic Acids Res. 2016; 44(W1):W272–6. https://doi.org/10.1093/nar/gkw398 PMID: 27185894

92. Bremer J, Granato M. Myosin phosphatase Fine-tunes Zebrafish Motoneuron Position during Axonogenesis. PLoS Genet. 2016; 12(11):e1006440. https://doi.org/10.1371/journal.pgen.1006440 PMID: 27855159

93. Soroldoni D, Hogan BM, Oates AC. Simple and efficient transgenesis with meganuclease constructs in zebrafish. Methods Mol Biol. 2009; 546:117–30. https://doi.org/10.1007/978-1-60327-977-2_8 PMID: 19378101